



Landslide hazard mapping using temporal probability analysis of rainfall thresholds in the city of Azazga and surrounding areas, northern Algeria

Hamid Bourenane¹

Received: 7 November 2022 / Accepted: 24 September 2023 / Published online: 6 October 2023
© Saudi Society for Geosciences and Springer Nature Switzerland AG 2023

Abstract

The main objective of this work is to evaluate the landslide hazard using temporal and spatial probability analysis at a large scale for the urban area of Azazga in northern Algeria. The historical landslide events for a period from 1952 to 2019 were collected and mapped from various sources, and a database was built. The daily and cumulative antecedent rainfall data related to landslide events were prepared from rain stations located in and around the urban area of Azazga. The rainfall threshold model for landslide occurrence was developed by analyzing the relationship between the daily and cumulative values of antecedent rainfall related to landslide events. The results show that 30-day antecedent rainfall is the most reliable predictor of current landslide events. The resultant rainfall threshold model was validated further using the 2012 rainfall and landslide events, which are not included in the threshold model. The results were used to estimate the temporal probability of a landslide occurrence using a Poisson probability model. For the spatial prediction probability of landslide initiation, four landslide susceptibility maps were previously prepared using statistical models. Finally, landslide hazard maps were produced by combining the temporal and spatial probabilities of landslides for three return periods: 1, 3, and 5 years. The obtained results could be considered as a first step toward reducing landslide risk and developing an early warning system.

Keywords Antecedent rainfall · Landslide hazard · Rainfall threshold · GIS · Algeria

Introduction

Rainfall-induced landslides, especially during the winter season, are the most recurrent geological hazards that have a high-risk impact in the Azazga urban area in northern Algeria. Rainfall was particularly heavy impact over the last decade, resulting in an increase in the frequency of landslides, which have caused significant damage to infrastructure, properties, forests, and agricultural areas (Djeral et al. 2014; Bourenane et al. 2021a, b). Landslides principally occur during rainy season between December and February, mainly during intense rainfall. The most recent cases occurred in 2012, 2014, and 2018 were caused and

reactivated by intense rainfall during the winter season, causing substantial and extensive damages at different parts of the Azazga urban area (Bourenane et al. 2021a, b, 2022a). Moreover, the extension of landslide events in the Azazga can be attributed to the effects of steep terrain, geological structures, mechanical characteristics of rock layers, tectonic activity, climate change, and extensive human activities. In addition, rapid and unplanned development of land-use planning in landslide-prone areas, territory mismanagement, and a lack of risk mitigation strategy exacerbate the impact of the landslide hazard and increase the risk. However, the landslide hazard was not adequately considered in the local development strategy and land use planning. Furthermore, despite the ongoing evolution of landslides and their associated adverse impacts, there has been virtually little studies that aims to predict and prevent these hazards (Djeral et al. 2014; Bourenane et al. 2021a, b, 2022a). Therefore, landslide hazard assessment and mapping are essential and urgent tasks that may assist authorities in reducing landslide damage through effective land use planning and development.

Responsible Editor: Biswajeet Pradhan

✉ Hamid Bourenane
b.hamid725@gmail.com

¹ Division Microzonage Sismique, Centre National de Recherche Appliquée en Génie Parasismique (CGS), 1 Rue Kaddour Rahim, Hussein Dey, Alger, Algeria

During the last decade, landslide hazard assessment has been recognized as an important research topic. The majority of the progress has been made in producing susceptibility and hazard maps at regional scales (1:25,000–1:50,000), while at large scales (1:10,000), used in land use rules, such studies are scarce. However, assessing landslide hazard and risk at a large scale using a minimal set of data, a replicable methodology, and geographical information systems (GIS) tools is a real challenge for earth scientists, risk managers, and government authorities.

Landslide hazard is defined as the probability of landslides of a given magnitude within a given area for a specified period of time (Varnes 1984; Van Westen et al. 2006). Landslide hazard mapping is associated with the division of an area into relatively homogeneous zones and their classification according to their degree of landslide hazard. Thus, landslide hazard integrates two main independent components: (1) location or “where” a landslide will occur (spatial probability) and (2) time or “when” or how frequently they will occur (temporal probability). Hence, landslide hazards assessment can be obtained from two sources: (i) landslide spatial probability, also known as landslide susceptibility, expressed as the spatial probability distribution of observed landslides in a territory for predisposing factors; and (ii) landslide temporal probability related to the occurrences of triggering events such as earthquakes and rainfalls.

For the evaluation of landslide hazards, different approaches and models have been effectively applied and developed in the literature (Guzzetti et al. 2006; Pradhan and Lee 2010; Pradhan 2012; Althuwaynee et al. 2012; Devkota et al. 2012; Lee et al. 2012; Pourghasemi et al. 2012a, b; Zare et al. 2012; Tien Bui et al. 2012; Pradhan et al. 2023). Nonetheless, there have been limited efforts made to estimate the temporal probability, mainly at a large scale due to the absence of historical datasets (Guzzetti et al. 2005; Jaiswal et al. 2010; Das et al. 2011). Thus, landslide hazard mapping is substantially difficult in poor countries, such as Algeria, due to insufficient datasets or the unavailability more of historical data.

Two methods have been largely used for the temporal probability assessment of future landslides. The first is the analysis of potential slope failure, while the second is the statistical analysis of past landslide events (Lopez Saez et al. 2012). The first method analyzes the local slope characteristics and estimates the probability of instability. This approach is less suitable for large areas because necessitating detailed knowledge of local conditions such as soil properties, shear parameters, changes in groundwater level, and discharge conditions (Jaiswal and van Westen 2009). The second examines the frequency of past landslide occurrences (Brabb 1984), which can be done directly using historical landslide records or indirectly using information from rainfall-triggered landslide events (Corominas and Moya

2008). Direct analyses of fairly extensive historical landslide data over a long-time range are thought to be a reliable way to determine the temporal probability. However, having such data for all of the current individual landslides on such a large scale is quite challenging. Therefore, an indirect method based on the rainfall frequency of occurrence was applied in this study to estimate the temporal probability of landslides. Although the indirect technique does not require a comprehensive multitemporal landslide inventory, it necessitates the development of accurate relationships between rainfall and the occurrence of landslides based on rainfall cluster times exceeding the threshold. Due to the fact that the frequency of rainfall-triggered landslides only offers an estimate of how frequently landslides may occur, it must be combined with the spatial prediction of potential landslides to produce a landslide hazard map (Corominas and Moya 2008).

Landslide hazard assessment using rainfall thresholds was performed with success in many areas throughout the world (Corominas and Moya 1999; Glade 2000; Chleborad 2000; Jakob and Weatherly 2003; Aleotti 2004; Coe et al. 2004; Guzzetti et al. 2005; Chleborad et al. 2006; Matsushi and Matsukura 2007; Salciarini et al. 2008, 2012; Martelloni et al. 2011; Melchiorre and Frattini 2012). Three main methods have been developed for determining rainfall thresholds, including physical-based threshold models, empirical models, and statistical models (Caine 1980; Wilson and Wiczorek 1995). The physical process models analyze the relationship between rainfall and local causal factors (such as lithology, slope gradient, and soil depth) using a dynamic hydrological model. Empirical models calculate rainfall thresholds by reviewing historical rainfall events that caused landslides. The thresholds are habitually determined by drawing lower bound lines in the graph of the plotted historical rainfall that induced landslides (Guzzetti et al. 2007). Statistical-based models use statistical analysis methods such as the logistic regression and the Bayesian inference to determine rainfall thresholds (Guzzetti et al. 2007; Frattini et al. 2009).

The goal of this research is to propose a reproducible methodology for evaluation and mapping landslide hazards using temporal and spatial probability analysis in the urban area of Azazga, northern Algeria. The methodology has been conducted, by using field data obtained from historical landslide records, including the dates of occurrence of the landslides and the daily rainfall records from five (5) rain gauge stations.

The temporal probability of a landslide was assessed using the Poisson model based on rainfall threshold. The rainfall threshold was calculated using a relationship between historical landslide records and the corresponding daily rainfall. The spatial probability analysis was evaluated using landslide susceptibility maps, which were produced

based on previous research by the same author using frequency ratio, statistical index, weights of evidence, and logistic regression models (Bourenane et al. 2021b). Subsequently, landslide hazard maps were produced by multiplying the temporal probability by the spatial probability. The final results give useful guidance for reducing landslide hazards and might be used as guidelines for landuse development planning in the city of Azazga.

Study area characteristics

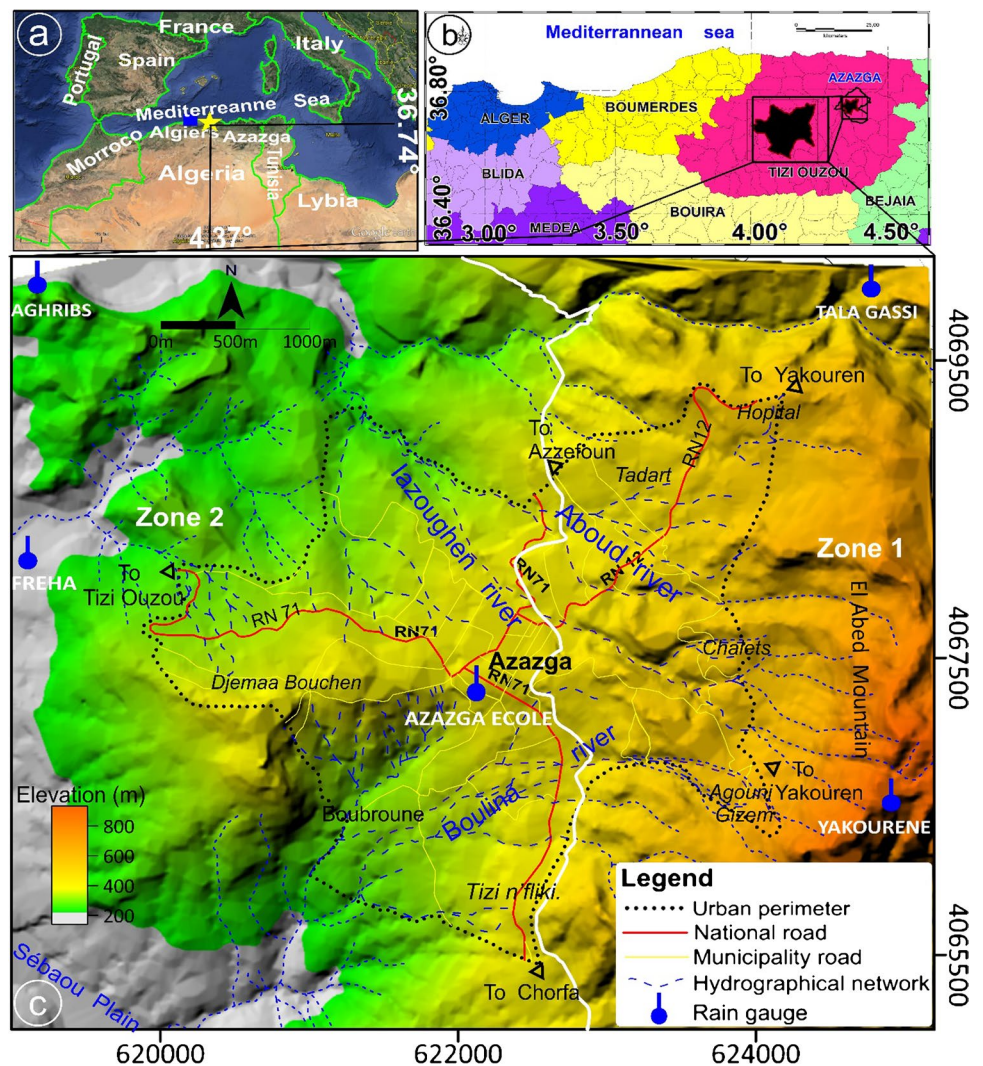
The Azazga region is geographically located in the northern region of Algeria (Fig. 1a), at about 35 km from Tizi-Ouzou Prefecture, and at about 135 km from the capital city, Algiers (Fig. 1b). The study area concerns the urban area of the city of Azazga, which is defined by its master plan (PDAU) perimeter (Fig. 1d), that covering a surface area of about 9 km². It is delimited by the longitudes of 619,620 m and

624,350 m and the latitudes of 4,065,390 to 4,069,450 m (WGS 1984 and UTM Zone 31, North).

Geomorphologically, the Azazga region is a part of the Great Kabylia Mountains that belong to the Tellian Atlas chain of northern Algeria. Three geomorphological units can be identified in the study area (Fig. 1 d): (i) the mountainous area of El Abed in the east with steep slopes and an altitude exceeding 700 m; (ii) the hilly area between the mountains and the valley where the altitudes are varying between 150 and 400 m; and (iii) the valley of Sébaou located at the western part of Azazga city with an altitude ranging between 50 and 150 m. The diverse topography makes the province one of the most susceptible regions in Algeria for natural disasters such as landslides. The elevation in Azazga City ranges from 500 to 1000 m above sea level and increases from the Southwest to the Northeast.

Geologically, the Azazga province is a part of the North Kabyle flysch domain that dominates the Neogene basin of Tizi-Ouzou to the west and limited to the south by the

Fig. 1 Geographical setting of the study area within (a) the north center of Algeria and located at the east of the capital city Algiers, (b) the north-east of the Tizi Ouzou prefecture with the administrative division of north Algeria, and (c) the administrative limit of the urban perimeter of the city of Azazga draped on the digital elevation model (DEM); the zones limit is categorized based on spatial coverage of rain gauges, rain gauge location, and elevation difference (the white line delimits the two zones)



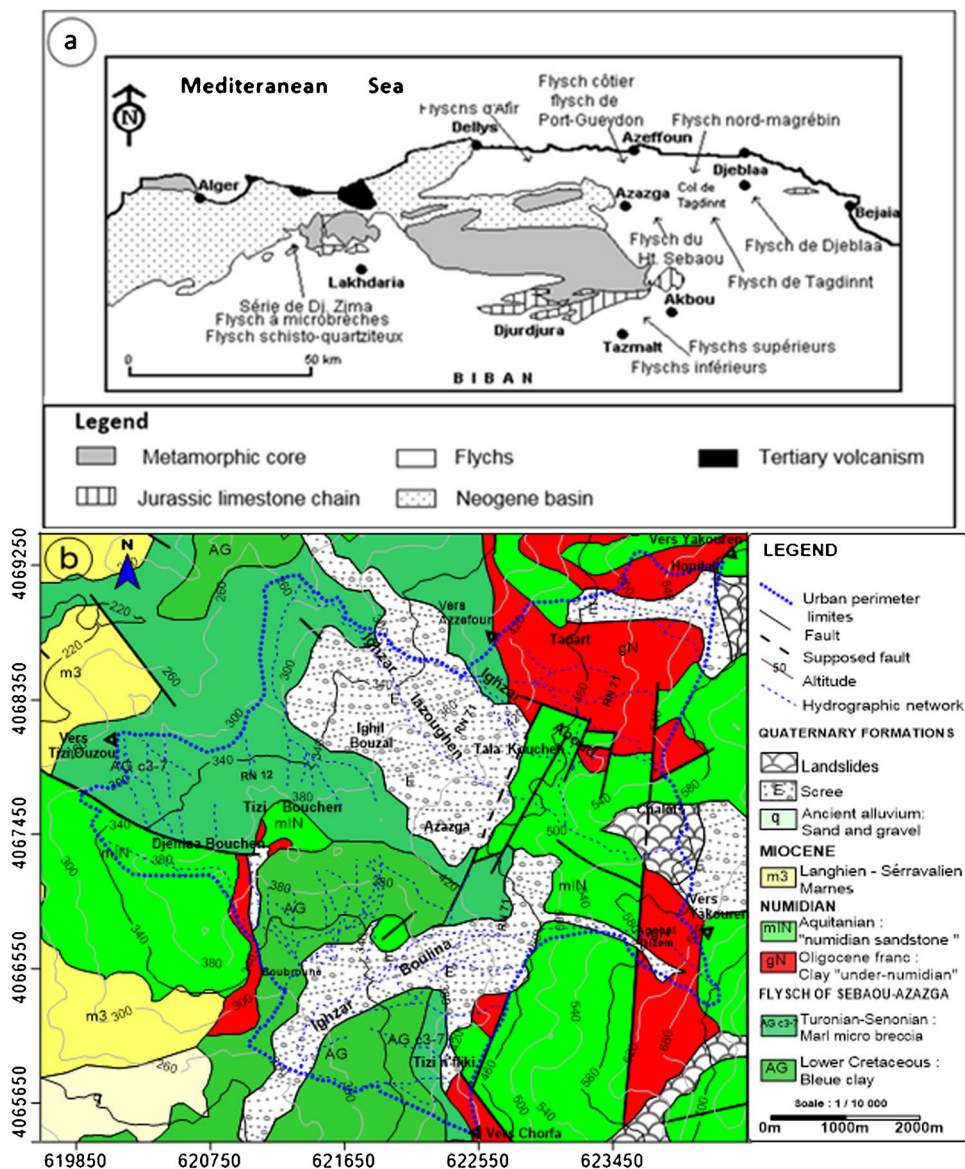
metamorphic core of Grande Kabylie and the Djurdjura Jurassic limestone chain (Raymond 1974; Wildi 1983) (Fig. 2a). The study area exhibits three main geological formations (Fig. 2b) (Gelard 1979; ORGM 1996): (i) the marly clays of the Cretaceous flysch in the western parts of Azazga City; (ii) the clays and the massive sandstones of the Oligocene Numidian flysch in the eastern parts; (iii) the clayed marls of the post-nappe Miocene in the NW; and (iv) the clayey and sandy sandstones of the Quaternary scree in the center and northern parts. Because of their high plasticity, these geological formations are highly susceptible to erosion, landslides, and flows in the presence of water.

Tectonically, the landslides are located in the faulted and folded flysch zone, a thrust sheet unit that experienced tectonic movements during the alpine cycle (Gelard 1979; ORGM 1996). The major tectonic characteristics include

(Fig. 2b) (i) a major tectonic contact, oriented N-S, dividing the “flysch of Azazga” unit and the Numidian unit; (ii) a system of faults oriented in two main directions, SW-NE, and NW–SE, visible especially in the Numidian sandstones; and (iii) overthrusting of the Numidian sandstones on the Cretaceous clay to the west.

The drainage network is represented by the semi-permanent flow of the Iazoughen, Aboud, and Boulina rivers, which are connected by a temporary flow affluent (Fig. 2b). The hydrogeology of the area is determined by the distribution of the permeable quaternary scree and the impermeable flysch substratum. The upper layer is permeable and allows water to pass through, while the underlying shale layer may be impermeable. The main aquifers are the Numidian sandstones and the Quaternary scree slopes. The slope’s water supply is replenished seasonally by rainfall via surface

Fig. 2 Geomorphological and geological setting of the study area: **a** geomorphological and structural positions of the flyschs in Greater Kabylia (Raymond 1974; Wildi 1983); **b** geological map of the Azazga region (ORGM 1996)



infiltration and fluctuates. As a result, groundwater is an important resource, particularly during the winter season (December to February), when rainfall is at its peak.

The land use of the urban area comprises settlement areas (46.5%), grass and agricultural land (34.5%), and forest (19%). The Azazga urban area is still developing and extending to forest and agricultural zones, which may lead to more frequent landslides.

The study area is situated in the Mediterranean climate type, characterized by dry seasons from June to September and rainy, snowy winters from October to April with a high frequency of intense rainfalls. According to the daily precipitation database from five rain gauges (Fig. 1 c) provided by the National Agency of Meteorology and Hydrology (ANRH) for a period of 67 years (1952–2019), the mean annual rainfall ranges from 1412 mm in the Aghrib and 1159 mm in the Yakourene regions (located in mountainous areas) to 723 mm in the Freha region, located in the plain area. The intermediate values of annual rainfall are recorded in the Azazga Ecole rain gauge (981 mm), located in a hilly area (Table 1). The frequency and intensity of the rainfall are focused mainly over a short period of time during the winter rainy season, which lasts from December to March and accounts for 50 to 60% of the yearly rainfall. The winter rainfall in Azazga can be characterized as being of low intensity, lasting a long time, and interrupted occasionally by bursts of heavy rain. During the winter and autumn seasons, highly variable rainfall quantities (700 to 1200 mm year⁻¹) occur with severe storms, causing a major landslide potential.

Data collection and database construction

Historical landslide inventory and mapping

The historical landslide inventory was performed for a period of 67 years, from 1952 to 2019. This map is based on landslide inventory maps from a variety of data sources, including (1) interpretation of aerial photographs, Google Earth satellite imagery, and high-resolution satellite imagery; (2) examination of historical landslide records

(landslide reports, newspaper records, and data collected from the field interviewing of local people); and (3) detailed and extensive fieldwork (Bourenane et al. 2021a, b). The database contains the in situ information associated with each landslide characteristic, such as the geological conditions of slopes, geomorphological features, and geometrical parameters, as well as the direct relationship with the rainfall amount, i.e., the temporal occurrence of rainfall-triggered landslides (Table 2).

Figure 3 depicts the spatial distribution of landslides in Azazga. The landslide perimeter occupies an area of about 2816 km², representing about 31% of the total urban area perimeter (master plan perimeter). The smallest landslide surface of the landslide is about 805 m², whereas the largest one is 6841 m². Since landslides are not evenly distributed throughout the study area, it is likely that lithology and other controlling factors play a significant role in determining when and where landslides occur.

According to Cruden and Varnes (1996) classification, the observed landslides can be divided into three types: (i) The slide represents an area of 27.95%; (ii) the flow represents 2.05%; and (iii) the rock falls with about a surface area of 1%. The flows are affected by rainfall events and actually occur during rainy seasons in less consolidated sandy clays, greatly altered, decompressed, and saturated on deep valleys and slopes with a mean slope of 20 to 30° along the Aboud river to the north and the Boulina river to the south of the city. The slides are the most important in terms of spatial extents and mobilized volumes. They are very common in the scree formations to the north of the city (Tadart, Tala Oukouchah, and Ighil Bouzal), along the Aboud and Boulina valleys, as well as in the Numidian clays to the east. The rock falls is the less common type and is mostly observed in the fractured Numidian sandstones in the mountains of the Djemâa-Bouchen in the west and the Djebel El Abed in the east of the urban area. This type is influenced by the sandstones' pre-existing fractures. The failures are caused by differential erosion or by the destabilization of the underlying formations when these sandstones alternate with marly or clayey soils.

According to an analysis of the relationships between the occurrence of landslides observed in the landslide inventory

Table 1 Available daily precipitation data (see Fig. 1c for the locations of the 05 meteorological stations) provided by the National Agency of Meteorology and Hydrology (ANRH)

N°	Meteorological station	Location			Daily rainfall data	Mean annual precipitation (mm)
		X (UTM)	Y (UTM)	Z		
1	AZAGA ECOLE	649.25	383.9	430	1950–2014	981.401
2	YAKOURENE	655.2	382.15	820	1950–2012	1159.054
3	TALA GASSI	654.6	389.45	560	1950–2012	1184.347
4	AGHRIBS	645.1	391.25	680	1950–2012	1412.457
5	FREHA	641.9	383.5	140	1950–2020	722.879

Table 2 Temporal occurrence of rainfall-triggered landslides in the city of Azazga from 1952 to 2019

Land-slide episode	Type of landslide	Date of occurrence (dd/mm/yyyy)	Daily rainfall (mm)	3 days rainfall (mm)	5 days rainfall (mm)	7 days rainfall (mm)	10 days rainfall (mm)	15 days rainfall (mm)	30 days rainfall (mm)	Affected areas
1	Flow	10/01/1952	29.2	114.6	155.1	199.5	230.3	311.2	721.7	Aït-Bouhimi in south east of the city of Azazga
2	Flow	18/02/1952	8.5	87.2	108.3	123.6	178.2	328.9	596.5	Djebel El Abed in south east of the city of Azazga
3	Slide	09/03/1952	17.3	51	105.3	129.2	161.2	216.4	501.7	Extension to the northern side of the Bouléna river
4	Flow	21/03/1955	20.9	19.8	69.6	81.5	129.9	177.8	382.9	Along Bouléna valley, in south of the city of Azazga
5	Slide	21/02/1973	42.3	73.3	114.4	127.8	160.2	189.8	260.3	Two landslides north of the city of Azazga: (1) at the ancient hospital and along RN 12 road, (2) Christian cemetery and along RN 12 road
6	Slide	06/04/1974	9.5	14.6	22.2	43.2	47.2	181.3	379.8	Reactivation and extension of landslides started in 1974 in many sites of the city of Azazga (Ighil Bouzel, Tizi Bouchen, Agoumi Guizem, Tala Oukouchah, and Taazibt)
7	Slide	21/03/1984	25.8	31	46.8	61	178	294.7	432.6	Ighil Bouzel, Agoumi Guizem, Tizi Bouchen, Tala Koucheh, and Taazibt
8	Slide	21/03/1985	5.4	38.7	51.4	66.9	93.9	249.5	364.8	
9	Slide	30/03/2002	24.4	13.7	23.6	26.8	52.5	96.4	229.6	Reactivation and extension of landslides started in 1974 and 1985
10	Slide	06/03/2003	8.8	22.7	43.2	50.3	62.1	137.2	400.5	Reactivations of landslides previously activated in 1974 and 1985 in north of the city: Ighil Bouzel, Tala-Oukouchah, l'Irhzer lazoughen, and Agoumi Guizem
11	Slide	01/03/2004	15.7	19.3	91.2	127.8	165.7	322.3	510.2	The new hospital, the site "les chalets," Boubroun in the south of the city
12	Slide	12/03/2006	13.3	111.2	256.2	265	275.5	318.7	422.1	The site of the new hospital
13	Slide	29/03/2008	23.6	28.8	88.4	90.6	97.6	148	417.8	Boubroun in the south of the city
14	Slide	16/12/2010	30.4	21.3	25.3	41.3	61.8	140.3	254.2	Along the RN12 road in the north of the city
15	Slide	07/03/2012	15.7	29.6	34.3	34.3	112.3	116.5	320.4	Ighil Bouzal, Tala Oukouchah, Ighil Bouzal, Zen, and Aït Bouhoumi
16	Slide	08/03/2012	35	64.6	69.3	69.3	147.3	151.5	355.4	Agoumi Guizem, Aït Bouhoumi
17	Slide	09/03/2012	21.8	70.7	89.4	91.1	120.1	173.2	377.2	Agoumi Guizem, Aït Bouhoumi
18	Slide	10/03/2012	36.5	36.5	36.5	37.3	37.3	105.4	354.4	Ighil Bouzal, Tala Oukouchah, Ighil Bouzal, Zen, and Aït Bouhoumi
19	Slide	11/03/2012	36.2	72.7	72.7	73.5	73.5	141.6	390.6	
20	Slide	21/01/2014	22.1	50.6	63.2	82.5	113.2	211.8	428.8	Tadart in NW of the city
21	Slide	11/03/2014	25.8	160.2	174.5	206.9	229.9	257	395.1	South of the new hôpital
22	Slide	10 /2/2014	33.9	52.2	128.3	154	169.7	218	418.7	City of 1er novembre in center of the city
23	Slide	11/02/2014	35.9	54.2	130.3	156	171.7	220	420.7	
24	Slide	13/03/2014	17.5	48.3	110.9	97.2	172.6	194.1	282.1	Tadart village, in NW of the city of Azazga
25	Slide	14/03/2014	30.8	48.5	93.4	79.7	155.1	176.6	264.6	
26	Slide	01/10/2015	8	32	32	32	32	32	54.8	

Table 2 (continued)

Land-slide episode	Type of landslide	Date of occurrence (dd/mm/yyyy)	Daily rainfall (mm)	3 days rainfall (mm)	5 days rainfall (mm)	7 days rainfall (mm)	10 days rainfall (mm)	15 days rainfall (mm)	30 days rainfall (mm)	Affected areas
27	Slide	21/06/2016	7.4	8.2	8.2	8.2	8.2	8.2	81.2	West of the city of Azazga
28	Slide	24/03/2018	32.8	47	64.4	68.7	68.7	84.9	210.7	Reactivation of landslides of 2012 and 2014
29	Slide	22/03/2018	32.8	47	64.4	68.7	68.7	84.9	210.7	Reactivation of landslides of 2012 and 2014
30	Slide	24/03/2018	60.3	70.6	109	126.4	130.7	140	237.9	Reactivation of landslides of 2012 and 2014
31	Slide	25/03/2018	24.3	87	89.3	89.3	97.9	136.1	426.5	Reactivation of landslides of 2012 and 2014
32	Slide	15/01/2019	6.2	62.7	65	65	73.6	111.8	402.2	West of the city of Azazga

map and each lithological unit, 65% of all landslides occur in the quaternary scree unit, followed by the cretaceous clay flysch unit, which accounts for 20%, and the numidian sandstone unit, which accounts for 25%. Regarding tectonics, the NW–SE and NE-SW fault directions appear to be in control of some landslides. The tectonic contacts between the Quaternary formations and the substratum, the fractures, and the schistosity planes in the slope direction create preferential flow drains that favor water infiltration and affect the occurrence of landslides.

The analysis of the landslide inventory indicates that the major part of the mass movements in the city of Azazga were generated by rainfall, which raised the pore-water pressure after infiltration into the soil. Referring to Table 2, the majority of these landslides occurred during rainy season, from October to April, when daily rainfall exceeded 8 mm. Though the antecedent rainfall that contributed to the saturation of the soil also had an essential influence on the landslide occurrences (Godt et al. 2006), numerous landslides occurred in January and March 1952, when daily rainfall and 3 days of antecedent rainfall exceeded 8.5 and 51 mm, respectively. A large number of landslide occurrences also occurred on March 24, 2018, when daily rainfall and 15-day antecedent rainfall exceeded 60 and 85 mm, respectively (Tables 1 and 2).

Rainfall distribution

Rainfall is largely regarded as the principal triggering factor of landslides in the city of Azazga and surrounding areas (Bourenane et al. 2021a). The historical landslide inventory conducted between 1952 and 2019 reveals that the primary causes of landslides are related to heavy rainfall events, with landslides principally occurring during the rainy season. In order to confirm this influence of rainfall events on landslides occurrence in the study area, the daily rainfall data from 1952 to 2019 was collected from the five (5) meteorological stations (Azazga Ecole, Yakourene, Tala Gassi Aghribs, and Freha) installed in and around the vicinity of the study area (Table 1 and Fig. 1c).

Analysis of the historical landslide inventory conducted from 1952 to 2019 indicates that the occurrence of landslides in the city of Azazga are typically linked to continuous and heavy rainfall events during the winter season from December and February (Fig. 4). The majority of historical landslide events observed in Azazga (1952, 1955, 1973, 1974, 1984, 2003, 2004, 2012, 2014, 2018, and 2019) are associated with high intensity of rainfall events that exceed 500 mm annually. Such a high intensity of rainfall can be enough to trigger landslides, nevertheless, the cumulative rainfall and antecedent rainfall also plays a crucial role in the initiation of the landslides.

Fig. 3 Landslide inventory map of the study area for the period of 67 years (1950–2019) used for the landslide hazard zonation. The numbering corresponds to the episode of the temporal occurrence of rainfall-triggered landslides data of Table 2

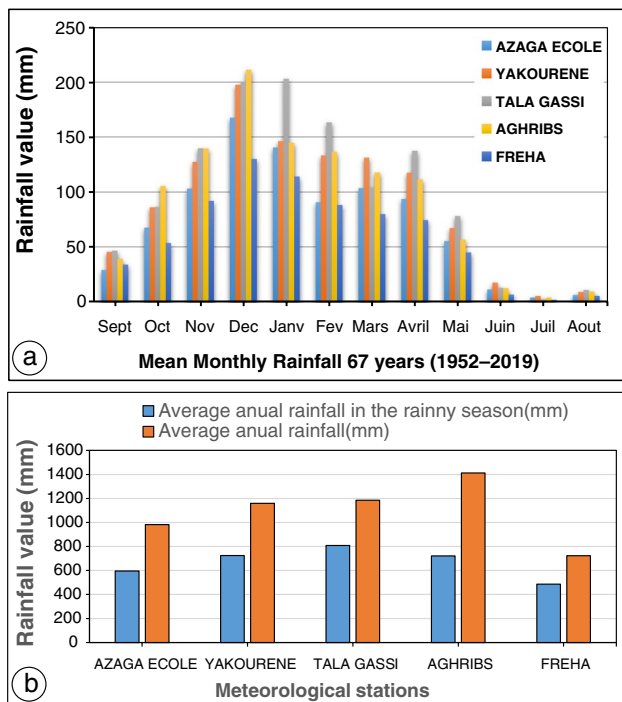
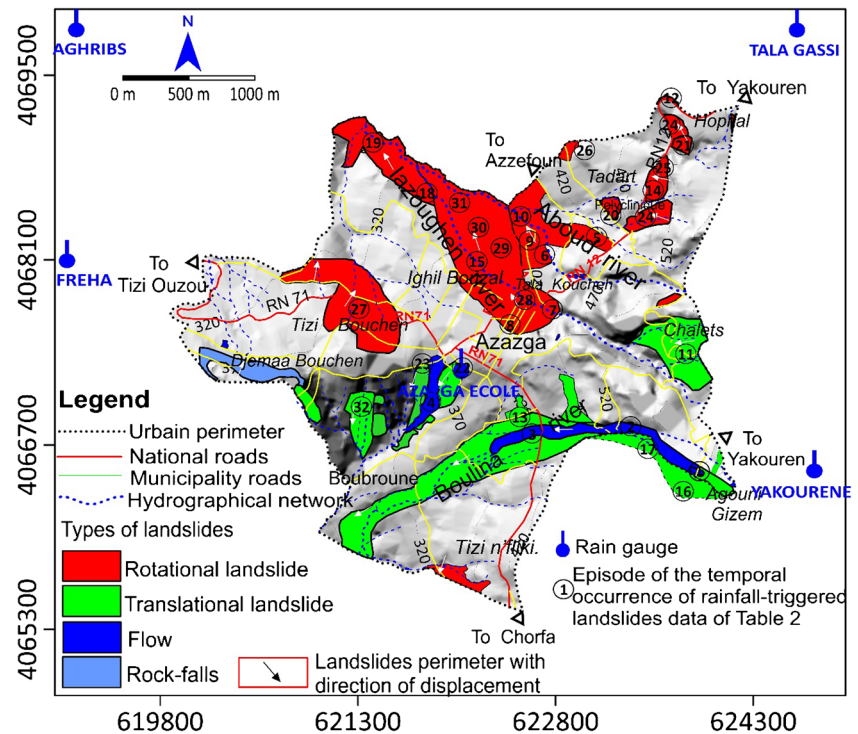


Fig. 4 Variation in rainfall distribution at five different rain gauges around Azazga for the period from 1952 to 2019. **a** Annual variation of monthly rainfall measures; **b** annual variation of annual rainfall measures

The annual rainfall distributions recorded at five stations clearly show a great variability and irregularity of the inter-annual rainfall as well as their extreme concentration over a specific period with an increase from downstream (plains) to upstream (mountains). Figure 4 depicts the annual variation in monthly (Fig. 4a) and annual rainfall (Fig. 4b) gathered from the rain gauges. This spatial distribution variability of precipitation is mainly related to the altimetric gradient with increasing rainfall from the Freha plain to the hilly areas (the town of Azazga) and the mountain areas (Yakourene and Aghribs). The average annual and rainy season precipitation was 1093 mm and 668 mm, respectively (Fig. 4). Monsoonal rainfall contributed 85% of the total rainfall during this period of time. The occurrence of these specific precipitation patterns proves the important role that rainfall plays in generating landslides in the study area. The mean annual rainfall ranges from 723 mm in the Freha region (Freha rain gauge) in the west of the city and 981.40 mm (Azazga Ecole rain gauge) in the center of the city to 1184.34 mm in the Aghrib region (Tala Gassi rain gauge) in the north (Table 1). The intermediate values of annual rainfall are recorded in the Yakourene region in the east, with annual rainfall ranging between 1159.05 mm (Yakourene rain gauge) and 1184.34 mm (Tala Gassi rain gauge). These results reflect the importance of torrential rains in the mountainous area.

Because of the variability of rainfall distribution, the study area is divided into two zones based on the spatial coverage of rain gauges, the location of the rain gauges, and elevation differences (Fig. 1c). Zone 1 concerns the eastern

part of the study area and represents the mountainous area with high slope (30° to 60°) where altitude can exceed 700 m. It houses two rain gauge stations, i.e., Yakourene and Tala Gassi. This area is underlain mostly by sandstones from the Oligocene Numidian Flysch. Zone 2 concerns the western and central parts of the study area and represents the hilly area with the gentle slope area (10° to 30°), and the altitudes are varying between 100 and 400 m. The zone houses two rain gauge stations: Azazga Ecole and Freha. This zone is represented by the sandy clays of Quaternary scree and the marly clays of the Cretaceous flysch.

The highest concentration of landslides or the landslide density is occurred during the highest rainfall where the antecedent rainfall influences the landslide occurrence (Table 2). Many landslides occurred in January 1952, when daily rainfall and 5 days antecedent rainfall exceeded 8.5 and 70 mm, respectively. A large number of landslide occurrences were also happened in March 2012, when daily rainfall and 15-day antecedent rainfall exceeded 22 and 105 mm, respectively. In March 2018, many slides occurred as a result of daily rainfall and 30-day antecedent rainfall exceeding 6.2 mm and 81.2, respectively (Table 2).

Temporal assessment of landslide hazard

Rainfall threshold estimation

Rainfall threshold, which corresponds to the minimum or maximum amount of rainfall required for landslide initiation in a specific area, is the principal independent component that contributes to the development of temporal probability (Guzzetti et al. 2007). Rainfall threshold is related to the limit of a hydrological condition that, when reached or exceeded, induces a landslide. The estimation of rainfall thresholds for landslide occurrence is considered a fundamental challenge in landslide hazard assessment. Many approaches have been presented and developed by various researchers to estimate rainfall thresholds (Dahal et al. 2009; Zezere et al. 2005; Giannecchini et al. 2012; Crosta 1998; Corominas and Moya 1999; D'Odorico and Fagherazzi 2003; Glade 2000; Frattini et al. 2009; Marques et al. 2008; Saito et al. 2010). They are classified into five threshold groups: (i) physical model; (ii) empirical; (iii) intensity duration; (iv) normalized intensity-duration; (v) cumulative rainfall; and (vi) antecedent rainfall. The rainfall intensity-duration thresholds and the empirical approaches are the most widely applied because they can easily and simply provide an approximate estimate of the minimum precipitation conditions. The most commonly used variables for estimating rainfall thresholds are daily rainfall, antecedent rainfall, cumulative rainfall, and normalized critical rainfall.

In the case of the study area, only the daily rainfall data is available; antecedent cumulative rainfall was considered to have a major role in the occurrence of landslides for the reason that it increases the pore-water pressure by reducing the shear strength of soil. As a result, the empirical method was used to establish the threshold model based on antecedent rainfall. Figure 2 illustrates the daily rainfall data recorded by each rainfall gauge station and nearby main landslide events in the Azazga between 1952 and 2019. Seasonal rainfall occurs with discontinuity and can be characterized as usually low-intensity, long-duration occurrences along with occasional extreme episodes, making the choice of antecedent rainfall suitable.

Antecedent rainfall is an essential factor in the initiation of landslides, particularly in less impermeable soils, as it reduces soil suction and increases pore water pressure. The most difficult part of using antecedent rainfall for landslide hazard estimation is determining the number of days to take into account. A thorough literature examination indicated a complex relationship between the number of days for the antecedent rainfall and the triggering of a landslide. Generally, the antecedent rainfall between 3 and 120 days was considered important in landslide occurrence understanding. The variation in the number of days for the antecedent rainfall can be influenced by a variety of factors, including (i) variation of the morphology, lithology, and vegetation; (ii) variation of meteorological and climatic conditions; and (iii) heterogeneity and incompleteness in the rainfall and landslide data used to determine the thresholds.

In order to estimate the number of days for the antecedent rainfall for this study, the inventory was categorized into two groups according to the two zones considered: zone 1 in the eastern part with a high slope and zone 2 in the western and central parts with a gentle slope (Fig. 1c). Then, we examined the relationship between the daily rainfalls and the related antecedent rainfall corresponding to the past landslide events for six periods: 3, 5, 7, 10, 15, and 30 days (Table 2). The results are shown in Fig. 5. The reliability results indicate the minimum number of rainfall days that have been plotted above each threshold (Lee et al. 2014). The red dots indicate the landslide events, whereas the blue dots represent the maximum yearly rainfall in 1 day without recorded landslides for the respective time periods. The best discrimination between events that induced landslides and those that did not was observed for the 30 days of antecedent rainfall. For the other antecedent rainfall days, discrimination appears to be less evident.

For this result, the rainfall threshold was estimated using the 30-day antecedent rainfall. For each zone, a scatter graph representing daily rainfall (with one or more landslides) against the corresponding 30-day antecedent rainfall was constructed to determine the rainfall threshold RTH. This graph is generated using historical rainfall-induced landslide

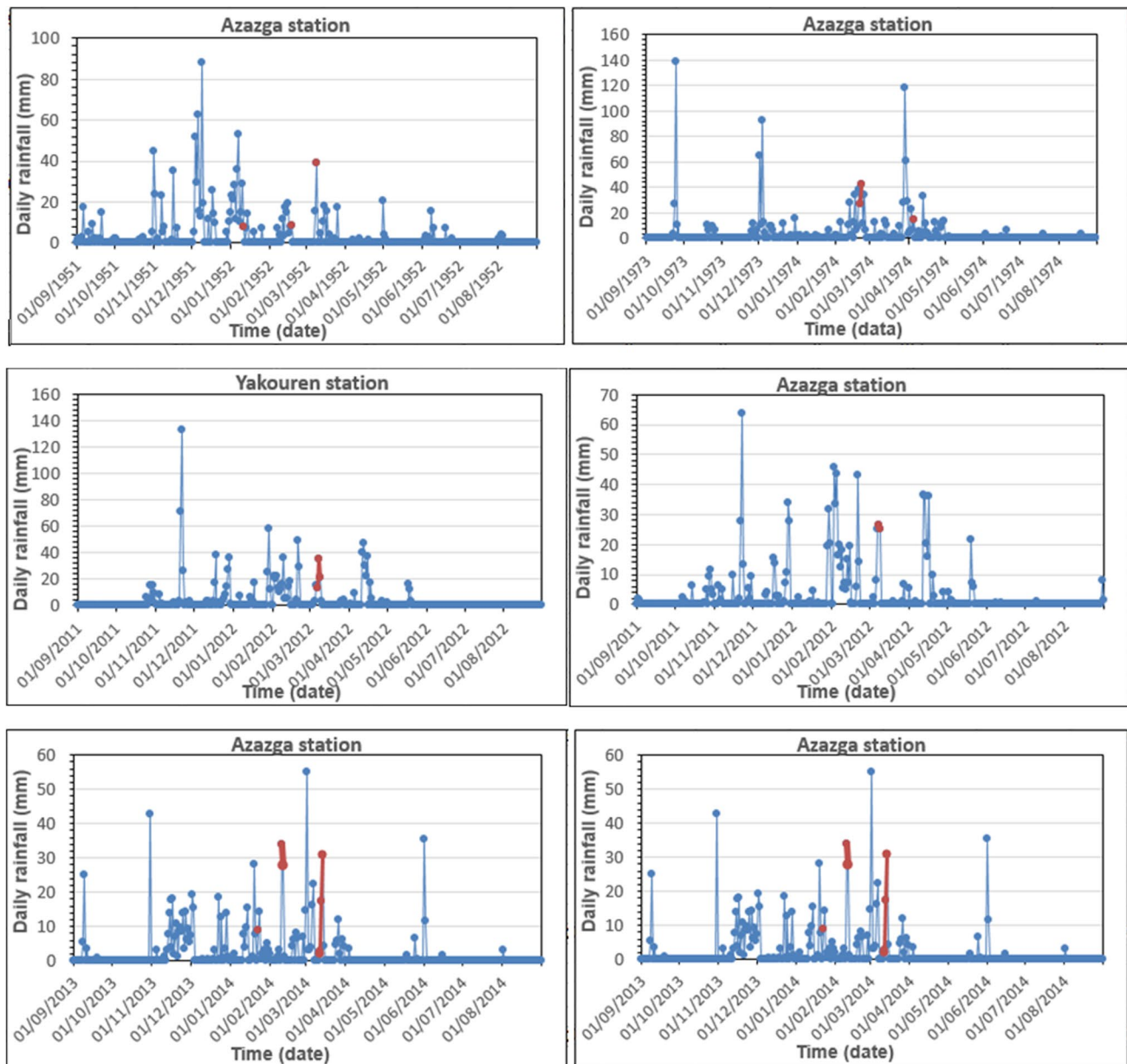


Fig. 5 Relationship between the daily rainfall (blue bars) recorded by each rainfall gauge station and the nearby main landslide events (red rounds) in the two defined zones

data from 1952 to 2019. The historical landslides of 2012 were used to validate the threshold. Figure 6 depicts the threshold equations, reliability values, and threshold values for each zone. Each zone has its own threshold based on the nearest event. Using the lower end of the plotted points in the scattered graph, the mathematical equation for the envelope curve for landslides was then obtained as RTH (zone 1) = $119.76 - 0.2115 R_{30Ad}$ and RTH (zone 2) = $72.303 - 0.1515 R_{30Ad}$, where RTH corresponds to the rainfall threshold and R_{30Ad} represents the cumulative rainfall values for the antecedent 30 days.

Validation of the rainfall threshold

The validation of the used models is regarded as the most important component in landslide hazard modeling, and without validation, the prediction models have no scientific importance (Chung and Fabbri 2003). Our rainfall threshold results in this study are validated by using recent rainfall events related to the landslide data for the period from 1 January 2012 to 31 December 2012. This dataset was not utilized in the development of the rainfall threshold model.

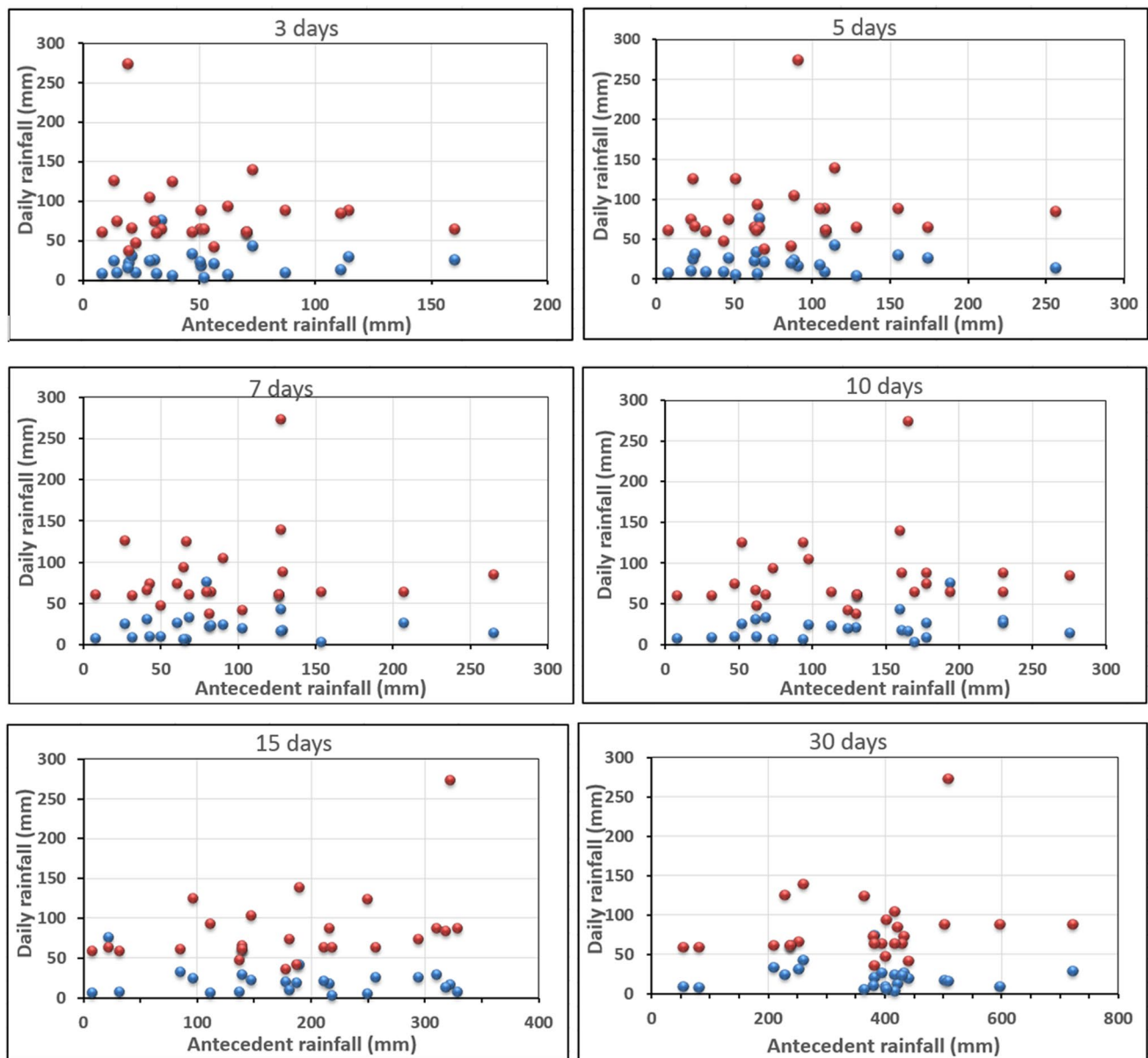


Fig. 6 Relationship between the daily rainfall and the antecedent rainfall in the city of Azazga for the period 1952–2019. In the figures, red diamonds depict the landslide events, and the blue diamond shows the maximum yearly rainfall in one day without a reported landslide

The result reveals that the rainfall threshold was exceeded several times in zone 1 and zone 2 during the period from January to December 2012 (Fig. 7). The threshold exceedance axis shows the value of RTH in relation to the value of R_{30Ad} for each day, with positive values indicating the occurrence of landslides. Figure 7 indicates that a heavy measure of rainfall occurred, exceeding the threshold. Successively, the rainfall threshold was exceeded 11 times in Yakouren (zone 1) and 23 times in Azazga (zone 2). It could be perceived that all landslides occurred when rainfall values exceeded these thresholds. In addition, other rainfall values that exceeded these thresholds have been recorded in the

two stations (Yakouren and Azazga), but no landslide was reported. The obtained results in this study indicated that all the used threshold models provided good accuracy in predicting landslide hazards in Azazga city.

Temporal assessment of landslide hazard

The estimation of the temporal probability of landslide hazard occurrence was based on the following two hypotheses: (1) the probability of landslide occurrence is associated with the probability of occurrence of the rainfall threshold (Jaiswal and van Westen 2009); and (2) the landslide will

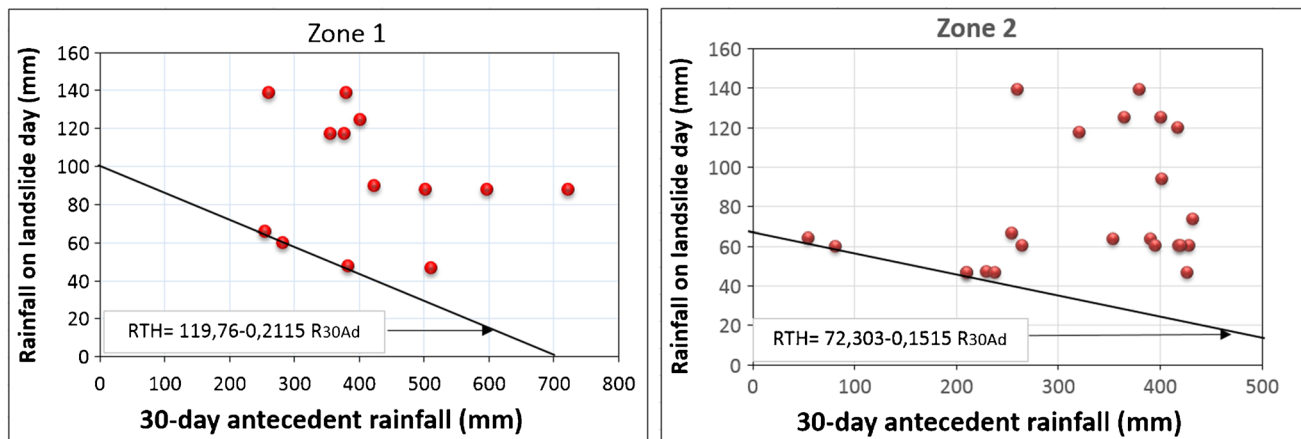


Fig. 7 Rainfall threshold for the city of Azazga, where RTH is the threshold rainfall, and R_{30Ad} is the 30-day antecedent rainfall

most likely occur when rainfall amounts exceed the rainfall threshold (Chleborad et al. 2006). For estimating the temporal probability of a landslide occurrence, the probability of occurrence of episodes of rainfall exceeding the rainfall threshold for the period of 67 years (from 1950 to 2019) was used based on a Poisson model, as follows (Crovelli 2000):

$$P(N(t) = n) = e^{-\lambda t} \frac{(\lambda t)^n}{n!}; n = 1, 2, 3, \dots \quad (1)$$

where $N(t)$ is the number of landslides that occurred during time t , and λ is the rate of n landslides occur.

The probability of one or more landslides occurring during time t , known as the exceedance probability, can be calculated as follows:

$$P(N(t) \geq 1) = 1 - \text{Exp}(-t/\mu) \quad (2)$$

where μ is the future mean recurrence interval and $\mu = t-1$; t is a future time period for which the exceedance probability is estimated. To estimate the future mean recurrence interval, we used the historical mean recurrence interval, with the supposition that the future landslides occurrence will be the same as it was in the past (Crovelli 2000).

The temporal probability of landslide hazards in the study area was obtained for the two defined zones individually, and their distribution along with the threshold equations is presented in Table 3. Initially, the number of times for which the threshold was exceeded for the study period (1952–2019) was calculated using the time series of daily rainfall from 5 rain gauges. Afterward, the temporal probability was calculated for three scenarios: 1, 3, and 5 years (Table 3). For zone 1, during the simulation period, the threshold value was exceeded 11 times, and out of these 11 cases, landslides were triggered in 10 cases. The estimated probability $P[L(R > RT)]$ for zone 1 was 0.90. The threshold value was also exceeded 23 and 64 times in zone 2 over the course of the 67-year period, triggering 14 landslides and adding 0.60 to the temporal probability values. The probability of at least one rainfall event occurring in any given year ranged from 0.60 to 0.90. The zone 1 received the highest probability values, followed by the zone 2. Additionally, this variation was observed in the number of landslide occurrences for each zone. During the monsoon season, these precipitation events were also capable of causing numerous landslides.

It is worth noting that, in some cases, rainfall days exceeding the threshold did not always result in a single landslide,

Table 3 Temporal probability of landslide hazard for the city of Azazga with the return periods of 1, 3, and 5 years

Zones	Threshold equation (RT)	A number of times the threshold are exceeded	P(R > RT)	Landslide frequency	P[L(R > RT)]	Temporal probability for different return periods		
						(1 year)	(3 years)	(5 years)
Zone 1 (Eastern part)	RTH = 119.76 - 0.2115 R30Ad	11	0.84	10	0.90	0.999	1	1
Zone 2 (center and Western part)	RTH = 72.303 - 0.1515 R30Ad	23	0.99	14	0.60	0.811	0.993	0.999

whereas moderate rainfall amounts triggered some landslide events. This scattered event occurred mostly in areas with gentle terrain (zone 2). This could be due to the following factors: (1) no extensive record of small events in the study area, (2) landslides caused by human activities, and (3) frequent and intense slope loading that initiates cracks and facilitates rainfall infiltration. The most frequently reported and destructive of human activities is road construction, which changes the landscape and accelerates the occurrence of slope instability (Chau et al. 2004).

Spatial prediction of landslide hazard

The spatial probability of landslide occurrence in a given area for a given conditioning factors is defined as landslide susceptibility, and its determination is one of the crucial steps needed to understand and identify potentially landslide prone sections for any study region. The spatial prediction of landslide susceptibility can be obtained by two basic categories of methods: (i) qualitative approaches based on expert knowledge of the target area, and (ii) quantitative approaches based on statistical algorithms. Since statistical techniques have produced completely satisfactory results over the past few decades, they are now viewed as being more objective and suitable for landslide susceptibility mapping, especially at large scales, due to their capacity to reduce the subjectivity in qualitative expert analysis.

Different landslide susceptibility maps (LSMs) were produced in the study area from earlier research by the same author using four statistical models, including frequency ratio (FR), statistical index (SI), weights of evidence (WoE), and logistic regression (LR) (Bourenane et al. 2021b). The evaluation and the mapping of landslide susceptibility are based on numerical expressions of the spatial statistical relationship between the distribution

of both landslide-conditioning factors and the landslides using GIS-based statistical modeling. For this objective, primarily, a landslide inventory map and ten landslide-conditioning factors (including the geology, distance to faults, distance to lineaments, precipitation, slope, altitude, aspect, land use, distance to drainage, and distance to roads) were prepared and derived from high-resolution satellite imagery and aerial photographs interpretation, detailed field observation, geological map, a DEM, and a rainfall database. Secondly, the susceptibility assessment was performed using four simple statistical models with the help of GIS techniques to generate LSMs. The assessment procedure is based on a cross-analysis of landslide-related factors and spatial frequency using statistical models and the GIS matrix method. The weighting factor values of the training sets of each layer for each landslide factor have been assessed using the equations of the four used models (FR, SI, LR, and WoE), in order to produce the final LSMs. The resulting maps (Fig. 8) were categorized into five distinct classes using the standard deviation method: low, moderate, high, and very high susceptibility. The total number of elements (weight value) was divided into these five groups. Finally, the obtained LSMs were validated using the ROC (receiver operating characteristic) curves. The ROC curves show that (Fig. 9) (i) all the statistical models provided good accuracy in landslide susceptibility mapping; and (ii) the landslide susceptibility model obtained from the frequency ratio (78.4%) has the highest prediction probability, followed by the statistical index (78.1%), weights of evidence (73.5%), and logistic regression (72.1%) models. The obtained maps were used in this study to determine the spatial probability of landslide hazards for the city of Azazga. The detailed application of the abovementioned four statistical models for landslide susceptibility mapping in the city of Azazga is described in previous work (Bourenane et al. 2021b).

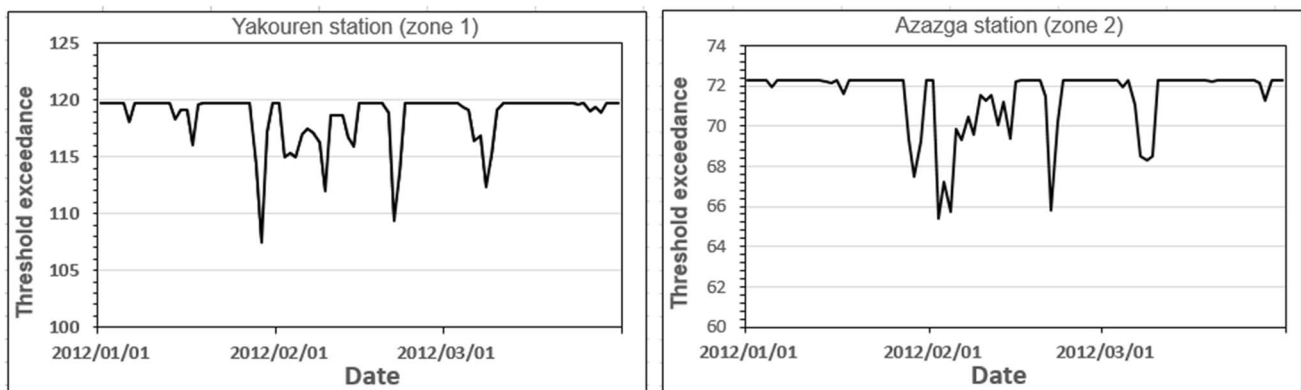


Fig. 8 Validation of the threshold models for the two defined zones in the city of Azazga. Positive values on the vertical axis indicate threshold exceedance (R [RTH])

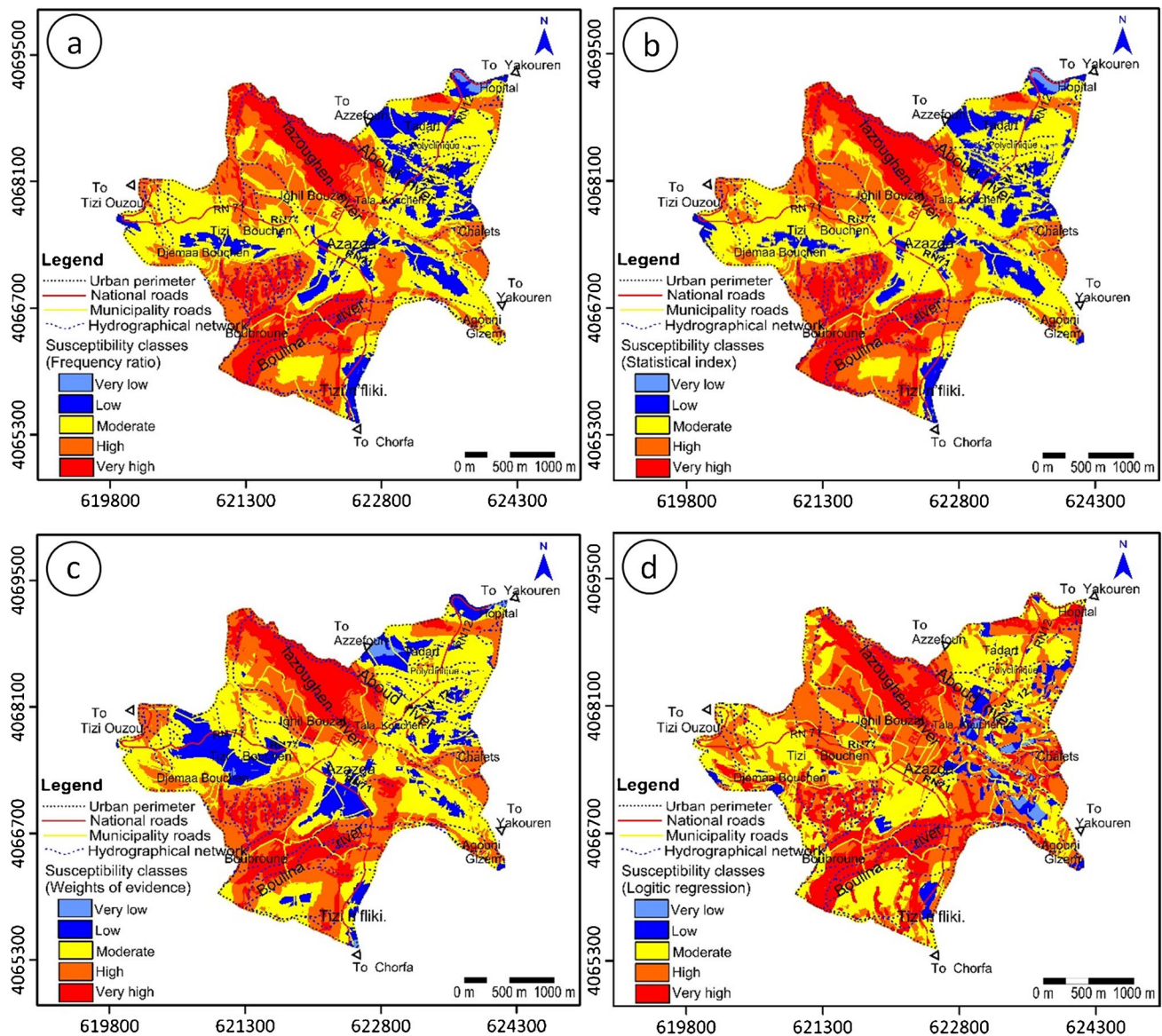


Fig. 9 Landslide susceptibility maps obtained from (a) the FR method; (b) the SI method; (c) the WoE method; and (d) the LR method (Bourneane et al. 2021b)

Landslide hazard assessment

The landslide hazard in the study area was evaluated by multiplying the temporal and spatial probability values of landslides for three return periods (1, 3, and 5 years) (Tien Bui et al. 2013). Twelve landslide hazard maps were produced and classified into five hazardous classes: very high, high, moderate, low, and very low. Examples of rainfall induced landslide hazard maps for the return periods of 1, 3, and 5 years are shown in Fig. 10. Figure 11 presents examples of detailed landslide hazard maps for three scenarios draped on high-resolution satellite images. For validation, the obtained landslide hazard maps have been compared with

the landslide inventory map using the statistical rules: first, the percentages of landslides increased concurrently with the degree of hazard and the observed landslide should belong to the high hazard class, and second, the high hazard class should cover only small areas (Bai et al. 2010). The results indicated that all the used models provided good accuracy in landslide hazard mapping in the city of Azazga. The cumulative percentage of landslides increased from a low-hazard zone to a very high hazard zone. Indeed, 60% of the landslide pixels are located in very-high hazard areas. Only a few landslide pixels (2%) are located in the very low-hazard areas. The landslide pixels falling in the moderate and low-hazard areas are 12% and 2%, respectively. Overall,

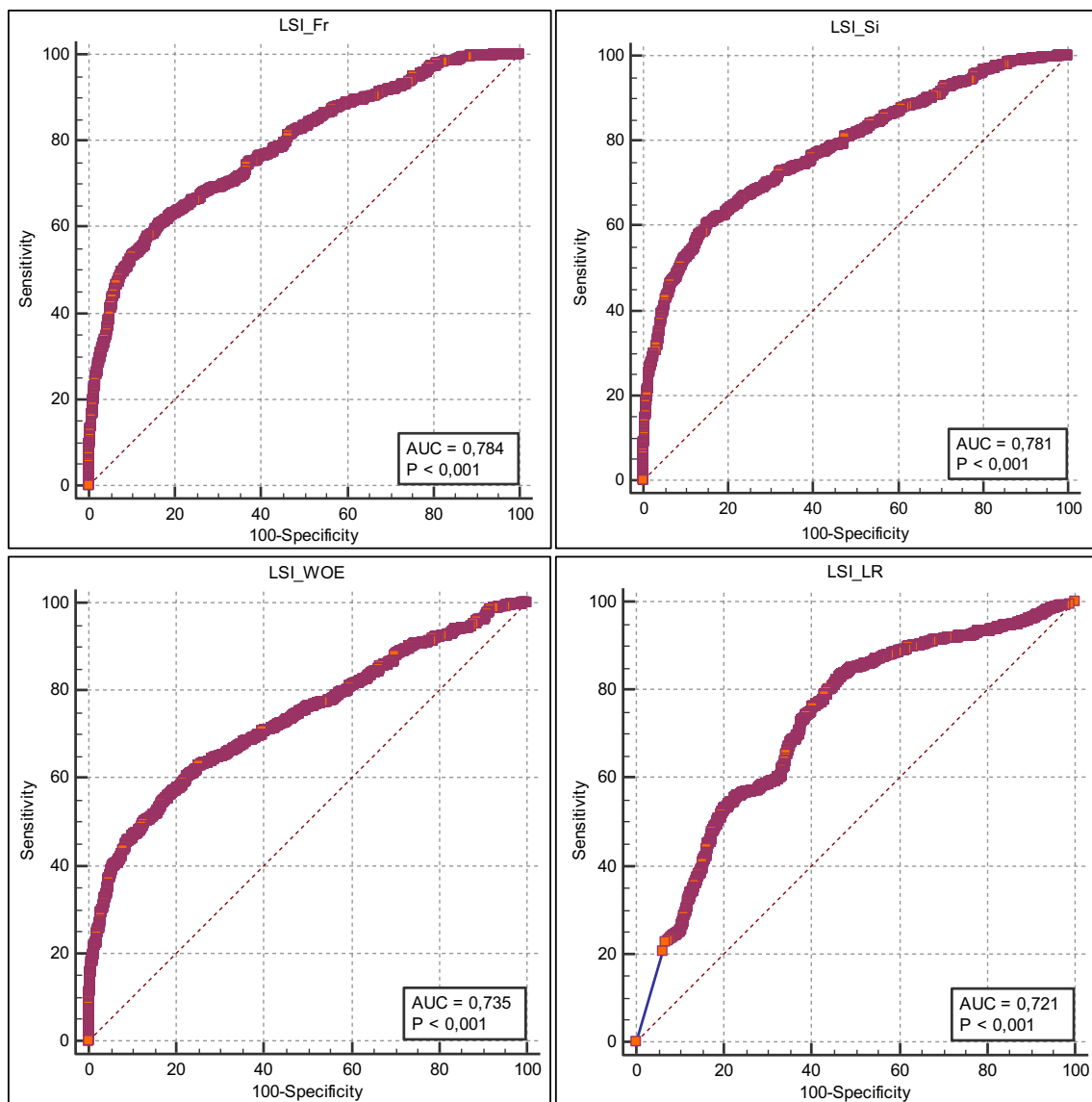


Fig. 10 Validation of the four statistical models (FR, SI, WoE, and LR) using the receiver operating characteristics (ROC) curves (Bourenane et al. 2021b)

the landslide hazard map clearly distinguishes between the very high and very-low hazard areas (Fig. 12). Furthermore, when planning mitigation and designing landslide remedial measures, the zone with a very high to moderate hazard should be considered.

Discussion

Landslides induced, especially during rainfall, are the most frequent natural hazard with a high-risk effect in the mountainous areas of Algeria (Bouhadad et al. 2010). The frequency of landslides has particularly increased over the last decade, due to heavy rainfall that has caused important

damage to constructions, infrastructures, and environmental areas. Therefore, assessing landslide hazards is a crucial and urgent task for authorities and a difficult challenge for scientists.

In the last decades, numerous methods and methodologies using statistical-based geospatial models combined with GIS technology have been developed for the quantitative assessment of landslide hazard; however, they may be best categorized as susceptibility models due to the fact that they only offer information on spatial probability (Das et al. 2011; Pradhan et al. 2023).

In this paper, we propose a methodology for landslide hazard assessment and mapping at large scales using a rainfall threshold model for landslide occurrence based on the

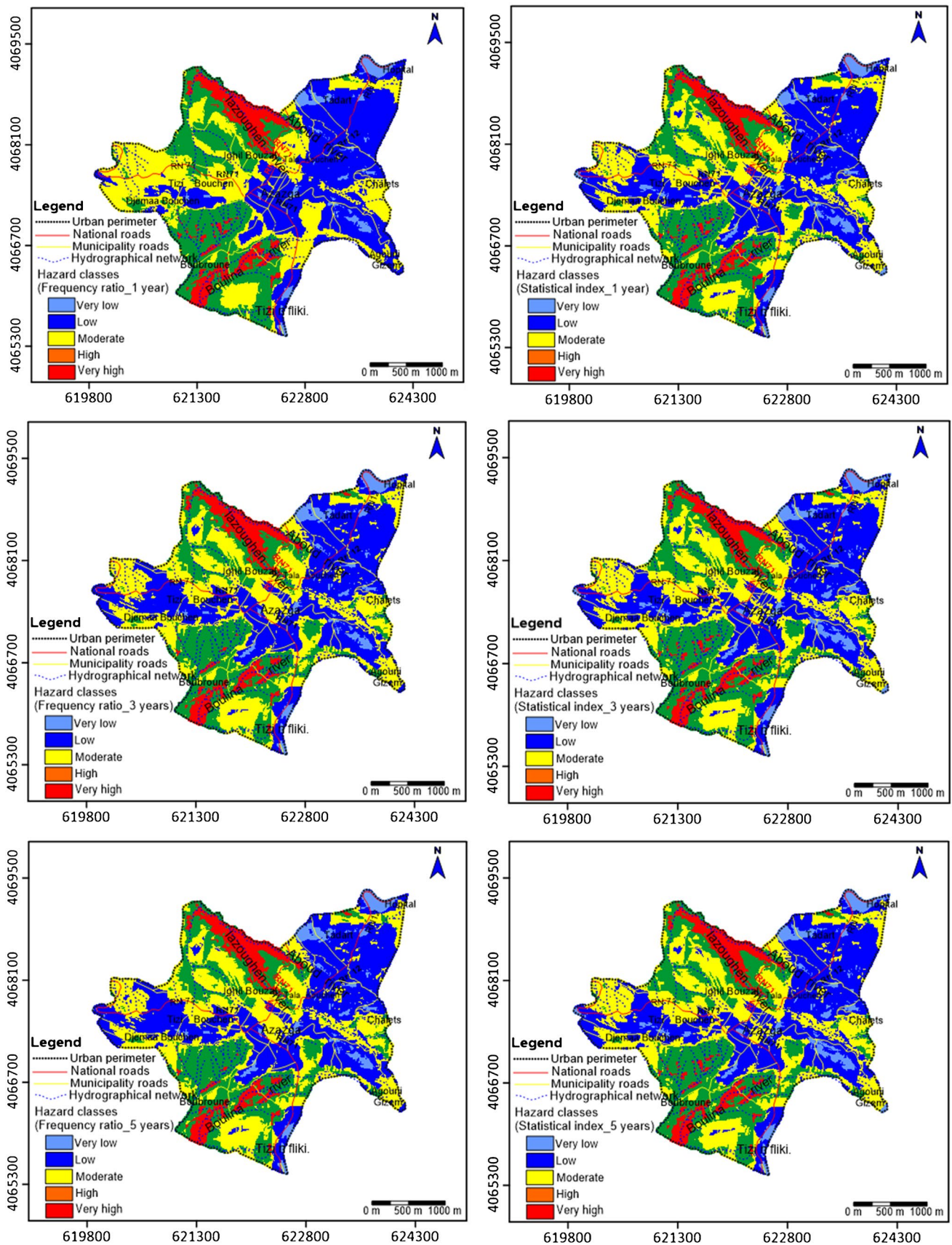
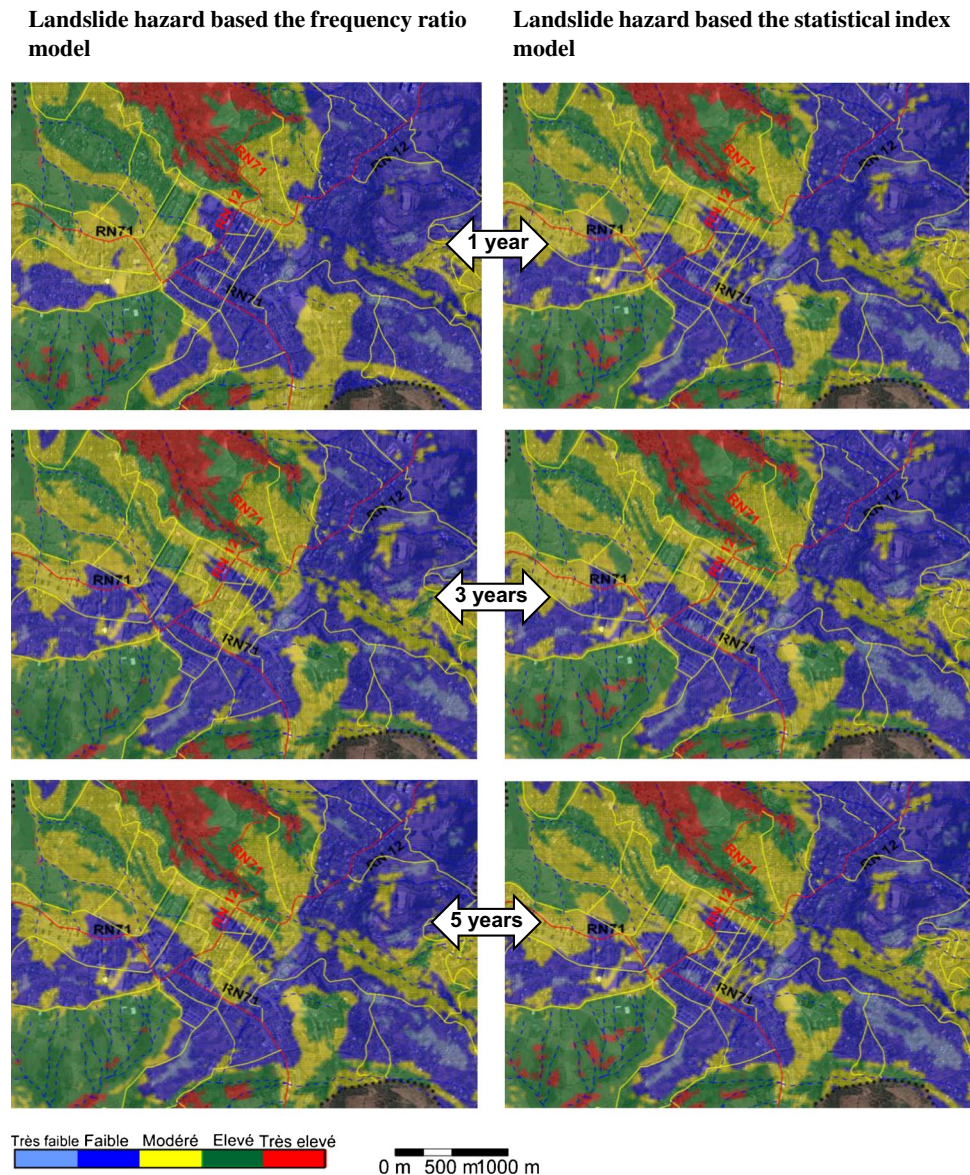


Fig. 11 Landslide hazard maps obtained from frequency ratio and statistical index for three scenarios 1, 2, and 5 years using the model

Fig. 12 Examples of detailed landslide hazard maps for three scenarios (return periods) 1, 2, and 5 years draped on high-resolution satellite images



relationship between the historical records and the related rainfall events. This methodology enables us to assess landslide hazard scenarios with available multi-temporal landslide inventories and daily rainfall records.

The landslide hazard maps were produced by combining the landslide susceptibility maps with the temporal probability of landslides. These hazard maps give information on the location “where” and time “when” a landslide will probably occur; as a result, land use planning for future development implementation in various scenarios (1, 3, and 5 years) is possible. The obtained landslide hazard maps can be used as a primary guide for comprehensive land use planning, urban development management at a detailed time and location.

The principal reasons for the scarcity of quantitative hazard assessment are represented by an insufficient inventory of the precise time and volume of landslides, the

classification of slope material failures, and an updated land use map. In this study, we filled a gap in the literature by generating a large-scale hazard map that includes the spatial and temporal aspects by using available information on rainfall-induced landslides from 1950 to 2019. Primarily, landslide susceptibility maps were established using geomorphological and geological conditioning factors that are unlikely to change during the prediction periods. Furthermore, other factors such as distance from roads and drainages, as well as land use, may be resistant to significant change after 5 to 10 years. However, we made sure to exclude the center of Azazga from a long-period prediction because its evolution is characterized by rapid development, increased deforestation, and infrastructural expansion. The spatial probability of the landslide (susceptibility) occurrence in the city is discussed comprehensively in Bourenane et al.

(2021b). The present paper focused only on the probability temporal and hazard map performances. The temporal probability of the landslides was estimated by an indirect method using the Poisson probability model by analyzing the relationship between the daily and cumulative or antecedent rainfall related to inventory landslide events.

The established landslide hazard maps show the spatial classification of areas into identical degrees of landslide hazard, from very high to very low-hazard. The detailed interpretation of the hazard map (example in Fig. 11) indicated areas with a high probability of landslides along the Aboud, Iazoughen, and Boulina river zones passing through the north and south of the city. They have been among the most susceptible zones in the study area to landslides in recent years. A very high-to-high probability of landslides is observed in other areas of the city of Azazga, such as Tala Oukouchah, Zen, and Ighil Bouzel, Agouni Guizem, and Ait Bouhouni, as shown in Fig. 11. A large historical landslide occurred in these areas (1952, 1955, 1973, 2004, 2012, 2014, 2018, and 2019), causing substantial damage to several constructions, national roads numbers 12 and 72, rural roads, and sensible infrastructures.

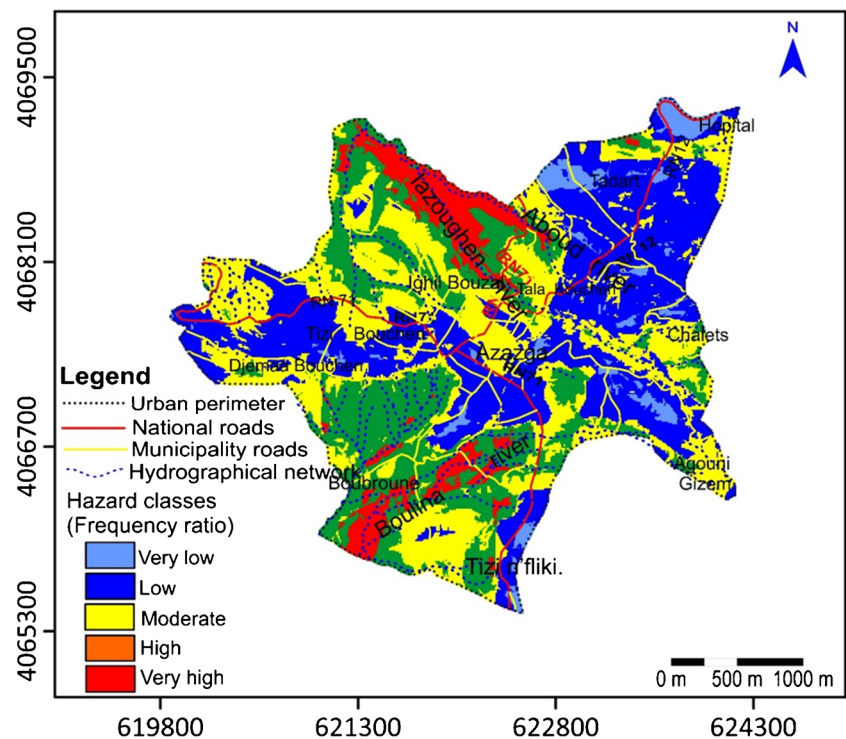
In relation to the vulnerable area, the resulted landslide hazard maps show that several high-risk zones are located within populated areas with extensive road networks and infrastructures (Figs. 10 and 11). This constitutes the main problem for landuse management and development in these areas. As shown on the map (Fig. 11), a high probability of landslide hazards has resulted in the loss

of properties and infrastructure because of recent landslides. Consequently, developing mitigation measures to reduce the impact of landslides should be prioritized in these areas.

In the city of Azazga, it is impossible to use traditional methods for direct analysis, that is, the frequency of landslides, to obtain landslide hazard maps because a full detail or complete temporal landslide is not available on a detailed landslide inventory map. Besides that, details on soil thickness and geotechnical properties are not available. For that reason, deterministic models for assessing the relative stability of slopes on a local scale are inapplicable in the studied area. As a result, the temporal probability of landslide occurrences was estimated using the indirect method based on the mean rate of occurrence of the rainfall threshold. This method is based on data on daily rainfall and the dates of landslide episodes over a 67-year period (1952–2019).

The comparison of the landslide hazard map and the landslide susceptibility maps reveals that some areas are relatively low susceptible to landslides (such as the Tizi Bouchen area in the city's west), but they become a little higher in landslide hazards (Fig. 13) at a given time in 1 year, and vice versa. This is due to the number of times rainfall has exceeded the period's average, resulting in a high temporal probability for those regions. Therefore, the probability of a landslide occurring in a particular area is a conditional function of the landslide susceptibility condition and the probability of a landslide-triggering rainfall event (Jaiswal et al. 2010).

Fig. 13 Landslide hazard map for the return period of 5 years based on the frequency ratio model



The spatial landslide hazard prediction models for Azazga urban area were built using the hypothesis that future landslides will occur under the same geo-environmental conditions as those that produced them in the past (Guzzetti et al. 2005). It is worth noting that the rainfall-triggering factor was not considered in the landslide susceptibility models. Given that the hazard models are predicted to be valid for 5 years, one might wonder if these factors will change during that time. It is reasonable to assume that in the research region, local characteristics such as lithology and faults will not change meaningfully over the time period under consideration. However, due to human activities, characteristics such as land use and distance to road will change during the next 5 years. This is due to the ongoing changes in the vegetation layer caused by clear-cut logging and deforestation in the catchment areas of the Boulina river, Iazoughen river, and Aboud river in the region. Additionally, the road network system has been expanded in recent years and will continue to be expanded in the future. As a result, several of the landslide conditioning variables included in the landslide susceptibility models may be modified. As a result, an evaluation of the change in land use and the road system during the considered time should be carried out. If the change is considerable on a local scale, the susceptibility models' conditioning factors of land use and distance to roadways should be revised. In Azazga, the temporal records of many landslides were not available. This absence in the landslide inventory leads to imprecision in hazard maps with respect to two points: (i) the relationship between landslide events and rainfall, and (ii) the rainfall that exceeded the threshold but did not result in a landslide event. These two factors tend to overestimate the probability of a long-time prediction (Jaiswal and van Westen 2009), such as over a period of 5 years.

The study area received the highest rainfall during the winter season; the eastern part, with its contrasted topography and rock formation, and the central and western parts, with their gentle terrain and soil formation, revealed variations in prediction probability despite receiving almost similar amounts of rainfall. This result comprehensively demonstrates that the occurrence of landslides is associated with the presence of contrasting terrain and geological formations (Guzzetti et al. 2008; Jaiswal et al. 2010; Malamud et al. 2004).

Because rainfall is the most common trigger factor for landslides, and there have been no reports of landslides induced by earthquakes in this region. The statistical correlation between historical rainfall and landslide incident data was used to estimate the temporal probability of landslides. The rainfall threshold was calculated by utilizing all landslide episodes without taking into account the specific size of the landslides or the number of landslides in the episodes. The effect of antecedent rainfall on triggering a landslide

was demonstrated. The results reveal that the cumulative rainfall for the antecedent period preceding the landslide triggering event should be considered for 15–30 days.

A comparison of the days of antecedent rainfall with those cited in the literature reveals that very diverse durations are taken into consideration in various empirical modeling methodologies, ranging from a few days to many months (Polemio and Sdao 1999). The determination of the number of days of antecedent rainfall is still difficult and dependent on local climate conditions, geology, slope, and physical–mechanical properties and permeability of soils (Aleotti 2004). In this study, a landslide inventory was only reported and recorded if it had a major impact on the infrastructure system. Furthermore, small landslides are not included in the landslide inventory map in tomporel terms. As a result, if the rainfall threshold is built for small landslides of different sizes independently, the temporal probability model may be improved.

This work presents an exhaustive understanding of the landslide hazard, causes, and effect relationships among various potential hazard factors in highly hazardous areas as useful information for developing a strategy for reducing the risk of a landslide in urban areas. The obtained landslide hazard maps constitute a valuable tool for making appropriate measures and decisions for landslide mitigation and prevention. The established landslide hazard maps in this work will give quantitative information on sites prone to landslides hazard in the future, assisting local authorities, planners, administrators, and decision-makers in infrastructure planning and development. As perspectives for future researches, the obtained results may serve to evaluate landslide vulnerability and risk.

Based on the obtained landslide hazard maps, the following mitigation measures may be suggested in order to reduce the impact of landslide hazard: (i) restricting development planning in the landslide-prone zones with the help of the obtained landslide hazard maps; (ii) requiring by means of codes the excavation, grading, landscaping, construction, vegetation clearance, and drainage control; (iii) protecting existing developments and the population by physical mitigation measures (drainage, counterfort, and protective barriers); (iv) developing and implementing monitoring and warning systems.

Conclusion

Azazga, in the mountainous province of Kabylia, is among the cities most heavily affected by the frequent landslide hazard caused by heavy rainfall. During the last decade, the intensity and impact of landslides have been significantly exacerbated by the rapid and uncontrolled expansion of urbanization in landslide-prone areas, the heavy

and prolonged rainfall trend, and the absence of hazard and risk mitigation strategies. Moreover, assessing and mapping landslide hazard is even more difficult in developed countries and is considered a high-priority scientific challenge.

This study evaluates the landslide hazard for the urban area of Azazga in northern Algeria based on a combination of the temporal probability analysis and the spatial probability at a large scale. The temporal probability was assessed by modeling the relationship between historical landslide records and the corresponding daily rainfall based on rainfall thresholds. The spatial probability analysis corresponds to the landslide susceptibility mapping, which is performed by using statistical modeling under GIS. Afterward, landslide hazard maps were generated by multiplying the spatial probability by the temporal probability. For this purpose, the methodology was carried out using field data acquired from historical landslide records, involving dates of landslide occurrence and daily precipitation records from rain gauge stations.

The historical landslide inventory map for a period from 1952 to 2019 was produced from Google Earth satellite images, historical records, and geological field investigations. The data concerning daily and antecedent rainfall related to landslide events were obtained from rain stations situated in and around the city of Azazga. The correlation between the daily and antecedent rainfall values was examined in order to develop the rainfall threshold model for the landslide occurrence. The results suggest that the most accurate predictor of existing landslide events is 30-day antecedent rainfall. The obtained results were used to evaluate the temporal probability of a landslide occurrence using a Poisson probability model. The results of the temporal probability were validated with a landslide event dataset from 2012 to understand the applicability of the model. For the spatial prediction of landslide occurrence, four landslide susceptibility maps were prepared using four statistical models, namely the frequency ratio, statistical index, weights of evidence, and logistic regression. The performance of the model was assessed using the area under the ROC, with a good accuracy achieved. Finally, landslide hazard maps were produced by combining the temporal probability and susceptibility of landslides for the return periods of 1, 3, and 5 years.

The predicted landslide hazard maps give helpful guidelines for reducing landslide risks and could serve as specifications for land use planning and development in the city of Azazga. The results could be seen as a first step in lowering risk and creating an early warning system.

Acknowledgements This research is supported by the National Center for Applied Research in Earthquake Engineering (CGS). The author wishes to express gratitude to the National Agency of Meteorology and Hydrology (ANRH) for providing the rainfall records of each rain gauge in the Azazga province. The author would like to express his gratitude to the respected Editor-in-Chief, Prof. Abdullah M. Al-Amri,

Prof. Biswajeet Pradhan, and all the anonymous reviewers for their valuable time and comments for upgrading the research work. The author also thanks everyone who provided assistance in the process of conducting this research. In addition, the author is grateful to Professor Bouhadad Youcef from CGS for his insightful criticism and English writing corrections.

Data Availability The data used in this research can be provided upon request from the corresponding author.

Declarations

Ethics approval Not applicable.

Consent to participate Not applicable.

Consent for publication Not applicable.

Competing interests The author declares no competing interests.

References

- Aleotti P (2004) A warning system for rainfall-induced shallow failures. *Eng Geol* 73(3–4):247–265. <https://doi.org/10.1016/j.enggeo.2004.01.007>
- Althuwaynee OF, Pradhan B, Lee S (2012) Application of an evidential belief function model in landslide susceptibility mapping. *Comput Geosci* (0). <https://doi.org/10.1016/j.cageo.2012.03.003>
- Bai S, Wang J, Lu G, Zhou P, Hou S, Xu S (2010) GIS-based logistic regression for landslide susceptibility mapping of the Zhongxian segment in the three Gorges area, China. *Geomorphology* 115:23–31
- Bouhadad Y, Benhammouche A, Bourenane H, Ait Ouali A, Chikh M, Guessoum N (2010) The Laalam (Algeria) damaging landslide triggered by a moderate earthquake (Mw = 5.2). *Nat Hazards* 54:261–272
- Bourenane H, Braham M, Bouhadad Y, Meziani AA (2021a) Spatial distribution, controlling factors and failure mechanisms of the large-scale landslides in the urban area of Azazga city (northern Algeria). *Environ Earth Sci* 80:313. <https://doi.org/10.1007/s12665-021-09607-5>
- Bourenane H, Meziani AA, Ait Benamar D (2021b) Application of GIS-based statistical modeling for landslide susceptibility mapping in the city of Azazga, Northern Algeria. *Bull Eng Geol Environ*. <https://doi.org/10.1007/s10064-021-02386-0>
- Bourenane H, Bensalem R, El Hadi O, Braham M, Meziani AA, Tebbouche MY (2022a) The large deep-seated landslide Induced by the March 12th, 2012 Rainfall Event in the City of Azazga, Northern Algeria: deformation characteristics and failure mechanisms. *Environ Earth Sci* 81:476. <https://doi.org/10.1007/s12665-022-10612-5>
- Brabb E (1984) Innovative approaches to landslide hazard mapping. In: *Proceedings of 4th international symposium on landslides, 1984. Canadian Geotechnical Society. Toronto, Canada*, pp 307–323
- Caine N (1980) The rainfall intensity-duration control of shallow landslides and debris flows. *Geografiska Annaler Ser a Phys Geogr* 62(1–2):23–27. <https://doi.org/10.2307/520449>
- Chau K, Sze Y, Fung M, Wong W, Fong E, Chan L (2004) Landslide hazard analysis for Hong Kong using landslide inventory and GIS. *Comput Geosci* 30:429–443
- Chleborad AF (2000) Preliminary method for anticipating the occurrence of precipitation-induced landslides in Seattle, Washington. US geological survey open-file report 00–0469

- Chleborad AF, Baum RL, Godt JW (2006) Rainfall thresholds for forecasting landslides in the Seattle, Washington, area-exceedance and probability. USGS open-file report 2006-1064
- Chung CJF, Fabbri AG (2003) Validation of spatial prediction models for landslide hazard mapping. *Nat Hazards* 30(3):451–472
- Coe JA, Michael JA, Crovelli RA, Savage WZ, Laprade WT, Nashem WD (2004) Probabilistic assessment of precipitation-triggered landslides using historical records of landslide occurrence, Seattle, Washington. *Environ Eng Geosci* 10(2):103. <https://doi.org/10.2113/10.2.103>
- Corominas J, Moya J (1999) Reconstructing recent landslide activity in relation to rainfall in the Llobregat River basin, Eastern Pyrenees, Spain. *Geomorphology* 30(1–2):79–93. [https://doi.org/10.1016/S0169-555X\(99\)00046-X](https://doi.org/10.1016/S0169-555X(99)00046-X)
- Corominas J, Moya J (2008) A review of assessing landslide frequency for hazard zoning purposes. *Eng Geol* 102(3–4):193–213. <https://doi.org/10.1016/j.enggeo.2008.03.018>
- Crosta G (1998) Regionalization of rainfall thresholds: an aid to landslide hazard evaluation. *Environ Geol* 35(2):131–145. <https://doi.org/10.1007/s002540050300>
- Crovelli RA (2000) Probability models for estimation of number and costs of landslides. United States geological survey open file report 00-249. <https://pubs.usgs.gov/of/2000/0249/report.pdf>
- Cruden DM, Varnes DJ (1996) Landslide types and processes. In: Turner AK, Schuster RL (eds) *Landslides: investigation and mitigation*, TRB special report, 247. National Academy Press, Washington, pp 36–75
- D’Odorico P, Fagherazzi S (2003) A probabilistic model of rainfall-triggered shallow landslides in hollows: a long-term analysis. *Water Resour Res* 39(9). <https://doi.org/10.1029/2002wr001595>
- Dahal R, Hasegawa S, Nonomura A, Yamanaka M, Masuda T, Nishino K (2009) Failure characteristics of rainfall-induced shallow landslides in granitic terrains of Shikoku Island of Japan. *Environ Geol* 56(7):1295–1310. <https://doi.org/10.1007/s00254-008-1228-X>
- Das I, Stein A, Kerle N, Dadhwal V (2011) Probabilistic landslide hazard assessment using homogeneous susceptible units (HSU) along a national highway corridor in the northern Himalayas, India. *Landslides* 8(3):293–308. <https://doi.org/10.1007/s10346-011-0257-9>
- Devkota K, Regmi A, Pourghasemi H, Yoshida K, Pradhan B, Ryu I, Dhital M, Althuwaynee O (2012) Landslide susceptibility mapping using certainty factor, index of entropy and logistic regression models in GIS and their comparison at Mugling–Narayanghat road section in Nepal Himalaya. *Nat Hazards*:1–31. <https://doi.org/10.1007/s11069-012-0347-6>
- Djeralb L, Alimrina N, Melbouci B, Bahar R (2014) Mapping and Management of Landslide Risk in the City of Azazga (Algeria) *Landslide Science for a Safer Geoenvironment* pp 463–468. https://doi.org/10.1007/978-3-319-05050-8_72
- Fratini P, Crosta G, Sosio R (2009) Approaches for defining thresholds and return periods for rainfall-triggered shallow landslides. *Hydrol Process* 23(10):1444–1460. <https://doi.org/10.1002/hyp.7269>
- Gelard JP (1979) *Géologie du Nord – Est de la Grande Kabylie (un segment des zones interne de l’orogène littoral maghrébin) – Thèse de doctorat*
- Gianacchini R, Galanti Y, Avanzi GD (2012) Critical rainfall thresholds for triggering shallow landslides in the Serchio River Valley (Tuscany, Italy). *Nat Hazards Earth Syst Sci* 12(3):829–842. <https://doi.org/10.5194/nhess-12-829-2012>
- Glade T (2000) Applying probability determination to refine landslide-triggering rainfall thresholds using an empirical “antecedent daily rainfall model”. *Pure Appl Geophys* 157(6):1059–1079. <https://doi.org/10.1007/s000240050017>
- Godt JW, Baum RL, Chleborad AF (2006) Rainfall characteristics for shallow landsliding in Seattle, Washington, USA. *Earth Surf Proc Land* 31(1):97–110. <https://doi.org/10.1002/esp.1237>
- Guzzetti F, Reichenbach P, Cardinali M, Galli M, Ardizzone F (2005) Probabilistic landslide hazard assessment at the basin scale. *Geomorphology* 72(1–4):272–299. <https://doi.org/10.1016/j.geomorph.2005.06.002>
- Guzzetti F, Reichenbach P, Ardizzone F, Cardinali M, Galli M (2006) Estimating the quality of landslide susceptibility models. *Geomorphology* 81(1–2):166–184. <https://doi.org/10.1016/j.geomorph.2006.04.007>
- Guzzetti F, Peruccacci S, Rossi M, Stark CP (2007) Rainfall thresholds for the initiation of landslides in central and southern Europe. *Meteorol Atmos Phys* 98(3):239–267. <https://doi.org/10.1007/s00703-007-0262-7>
- Guzzetti F, Peruccacci S, Rossi M, Stark C (2008) The rainfall intensity–duration control of shallow landslides and debris flows: an update. *Landslides* 5(1):3–17. <https://doi.org/10.1007/s10346-007-0112-1>
- Jaiswal P, van Westen CJ (2009) Estimating temporal probability for landslide initiation along transportation routes based on rainfall thresholds. *Geomorphology* 112(1–2):96–105. <https://doi.org/10.1016/j.geomorph.2009.05.008>
- Jaiswal P, van Westen CJ, Jetten V (2010) Quantitative landslide hazard assessment along a transportation corridor in southern India. *Eng Geol* 116(3–4):236–250. <https://doi.org/10.1016/j.enggeo.2010.09.005>
- Jakob M, Weatherly H (2003) A hydroclimatic threshold for landslide initiation on the North Shore Mountains of Vancouver, British Columbia. *Geomorphology* 54(3–4):137–156. [https://doi.org/10.1016/S0169-555X\(02\)00339-2](https://doi.org/10.1016/S0169-555X(02)00339-2)
- Lee ML, Ng KY, Huang YF, Li WC (2014) Rainfall-induced landslides in Hulu Kelang area, Malaysia. *Nat Hazards* 70:353–375
- Lee M-J, Choi J-W, Oh H-J, Won J-S, Park I, Lee S (2012) Ensemble-based landslide susceptibility maps in Jinbu area, Korea. *Environ Earth Sci* 1–15. <https://doi.org/10.1007/s12665-011-1477-y>
- Lopez Saez J, Corona C, Stoffel M, Schoeneich P, Berger F (2012) Probability maps of landslide reactivation derived from tree-ring records: Pra Bellon landslide, southern French Alps. *Geomorphology* 138(1):189–202. <https://doi.org/10.1016/j.geomorph.2011.08.034>
- Malamud BD, Turcotte DL, Guzzetti F, Reichenbach P (2004) Landslide inventories and their statistical properties. *Earth Surf Process Landf* 29:687–711
- Marques R, Ze’zere J, Trigo R, Gaspar J, Trigo I (2008) Rainfall patterns and critical values associated with landslides in Povoacão County (São Miguel Island, Azores): relationships with the North Atlantic Oscillation. *Hydrol Process* 22(4):478–494. <https://doi.org/10.1002/hyp.6879>
- Martelloni G, Segoni S, Fanti R, Catani F (2011) Rainfall thresholds for the forecasting of landslide occurrence at regional scale. *Landslides* 1–11. <https://doi.org/10.1007/s10346-011-0308-2>
- Matsushi Y, Matsukura Y (2007) Rainfall thresholds for shallow landsliding derived from pressure-head monitoring: cases with permeable and impermeable bedrocks in Boso Peninsula, Japan. *Earth Surf Proc Land* 32(9):1308–1322. <https://doi.org/10.1002/esp.1491>
- Melchiorre C, Fratini P (2012) Modelling probability of rainfall-induced shallow landslides in a changing climate, Otta, Central Norway. *Clim Change* 113(2):413–436. <https://doi.org/10.1007/s10584-011-0325-0>
- ORGM (1996) Geological map at scale of 1/50. 000, Publ. Service Géologique. Algérie
- Polemio M, Sdao F (1999) The role of rainfall in the landslide hazard: the case of the Avigliano urban area (Southern Apennines, Italy). *Eng Geol* 53(3–4):297–309. [https://doi.org/10.1016/S0013-7952\(98\)00083-0](https://doi.org/10.1016/S0013-7952(98)00083-0)
- Pourghasemi H, Pradhan B, Gokceoglu C (2012a) Application of fuzzy logic and analytical hierarchy process (AHP) to landslide

- susceptibility mapping at Haraz watershed, Iran. *Nat Hazards* 63(2):965–996. <https://doi.org/10.1007/s11069-012-0217-2>
- Pourghasemi HR, Mohammady M, Pradhan B (2012b) Landslide susceptibility mapping using index of entropy and conditional probability models in GIS: Safarood Basin, Iran. *Catena* 97:71–84. <https://doi.org/10.1016/j.catena.2012.05.005>
- Pradhan B (2012) A comparative study on the predictive ability of the decision tree, support vector machine and neuro-fuzzy models in landslide susceptibility mapping using GIS. *Comput Geosci*. <https://doi.org/10.1016/j.cageo.2012.08.023>
- Pradhan B, Lee S (2010) Landslide susceptibility assessment and factor effect analysis: backpropagation artificial neural networks and their comparison with frequency ratio and bivariate logistic regression modelling. *Environ Modell Softw* 25(6):747–759. <https://doi.org/10.1016/j.envsoft.2009.10.016>
- Pradhan B, Dikshit A, Lee S, Kim H (2023) An explainable AI (XAI) model for landslide susceptibility modeling. *Appl Soft Comput* 42:110324
- Raymond D (1974) Evolution sédimentaire et tectonique du Nord – Ouest de la Grande Kabylie (Algérie) au cours du cycle Alpin – Thèse de doctorat, sciences naturelles, Université Pierre et Marie Curie (Paris VI), département de géologie Structurale
- Saito H, Nakayama D, Matsuyama H (2010) Relationship between the initiation of a shallow landslide and rainfall intensity–duration thresholds in Japan. *Geomorphology* 118(1–2):167–175. <https://doi.org/10.1016/j.geomorph.2009.12.016>
- Salciarini D, Godt JW, Savage WZ, Baum RL, Conversini P (2008) Modeling landslide recurrence in Seattle, Washington, USA. *Eng Geol* 102(3–4):227–237. <https://doi.org/10.1016/j.enggeo.2008.03.013>
- Salciarini D, Tamagnini C, Conversini P, Rapinesi S (2012) Spatially distributed rainfall thresholds for the initiation of shallow landslides. *Nat Hazards* 61(1):229–245. <https://doi.org/10.1007/s11069-011-9739-2>
- Tien Bui D, Pradhan B, Lofman O, Revhaug I, Dick OB (2012) Landslide susceptibility mapping at Hoa Binh province (Vietnam) using an adaptive neuro-fuzzy inference system and GIS. *Comput Geosci* 45:199–211. <https://doi.org/10.1016/j.cageo.2011.10.031>
- Tien Bui D, Pradhan B, Lofman O, Revhaug I, Dick ØB (2013) Regional prediction of landslide hazard using probability analysis of intense rainfall in the Hoa Binh province, Vietnam. *Nat Hazards* 66:707–730. <https://doi.org/10.1007/s11069-012-0510-0>
- Van Westen CJ, Van Asch TWJ, Soeters R (2006) Landslide hazard and risk zonation—why is it still so difficult? *Bull Eng Geol Env* 65:167–184. <https://doi.org/10.1007/s10064-005-0023-0>
- Varnes DJ (1984) Landslide hazard zonation: a review of principles and practice. UNESCO, Paris
- Wildi W (1983) La chaîne tello-rifaine (Algérie, Maroc, Tunisie): Structure, Strati-Graphie et évolution du Trias au Miocène. *Rev Géol Dynam Géog Phys* 24:201–297
- Wilson RC, Wieczorek GF (1995) Rainfall thresholds for the initiation of debris flows at La Honda, California. *Environ Eng Geosci* 1(1):11–27
- Zare M, Pourghasemi H, Vafakhah M, Pradhan B (2012) Landslide susceptibility mapping at Vaz Watershed (Iran) using an artificial neural network model: a comparison between multilayer perceptron (MLP) and radial basic function (RBF) algorithms. *Arabian J Geosci* 1–16. <https://doi.org/10.1007/s12517-012-0610-x>
- Zeze JL, Trigo RM, Trigo IF (2005) Shallow and deep landslides induced by rainfall in the Lisbon region (Portugal): assessment of relationships with the North Atlantic Oscillation. *Nat Hazards Earth Syst Sci* 5(3):331–344

Springer Nature or its licensor (e.g. a society or other partner) holds exclusive rights to this article under a publishing agreement with the author(s) or other rightsholder(s); author self-archiving of the accepted manuscript version of this article is solely governed by the terms of such publishing agreement and applicable law.